

Gold Nanoparticles

Marie-Christine Daniel and Didier Astruc*

Chem. Rev. **2004**, *104*, 293-346

Scanometric DNA Array Detection with Au Nanoparticle Probes

Detection of Cancer cells at very early stage.

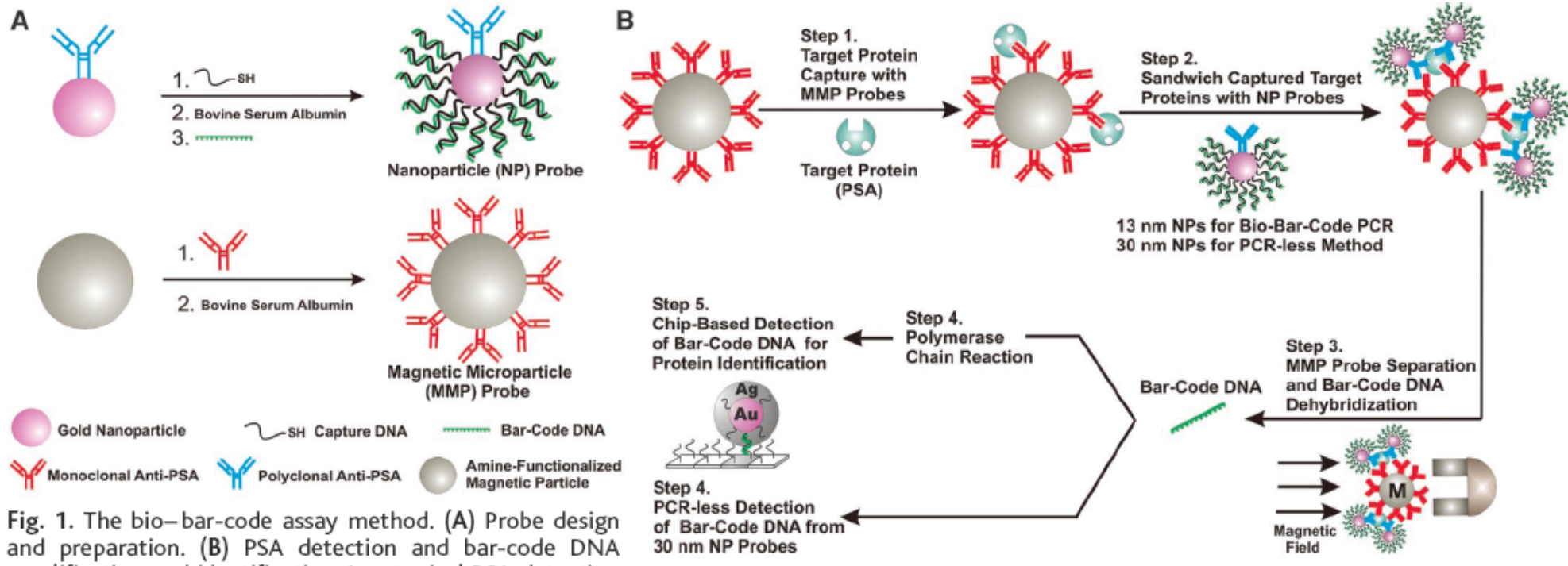
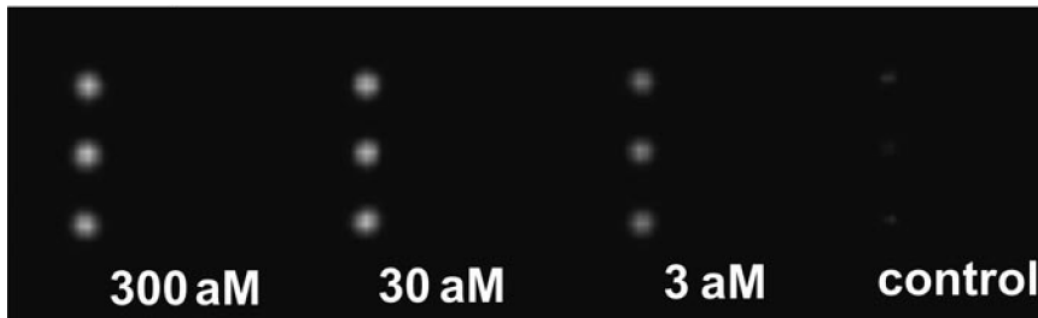


Fig. 1. The bio-bar-code assay method. (A) Probe design and preparation. (B) PSA detection and bar-code DNA



J.-M. Nam, C. S. Thaxton, C. A. Mirkin *Science* **2003**, 301, 1884.

T. Andrew Taton, 1,2 Chad A. Mirkin, 1,2* Robert L. Letsinger 1* *Science* **2000**, 289, 1757.

The Impact of Nanoscience on Heterogeneous Catalysis

Alexis T. Bell, *Science* **2003**, 299, 1688.

- [10] a) M. Haruta, S. Tsubota, T. Kobayashi, H. Kageyama, M. J. Genet, B. Delmon, *J. Catal.* **1993**, 144, 175–192; b) M. Haruta, M. Daté, *Appl. Catal. A* **2001**, 222, 427–437.

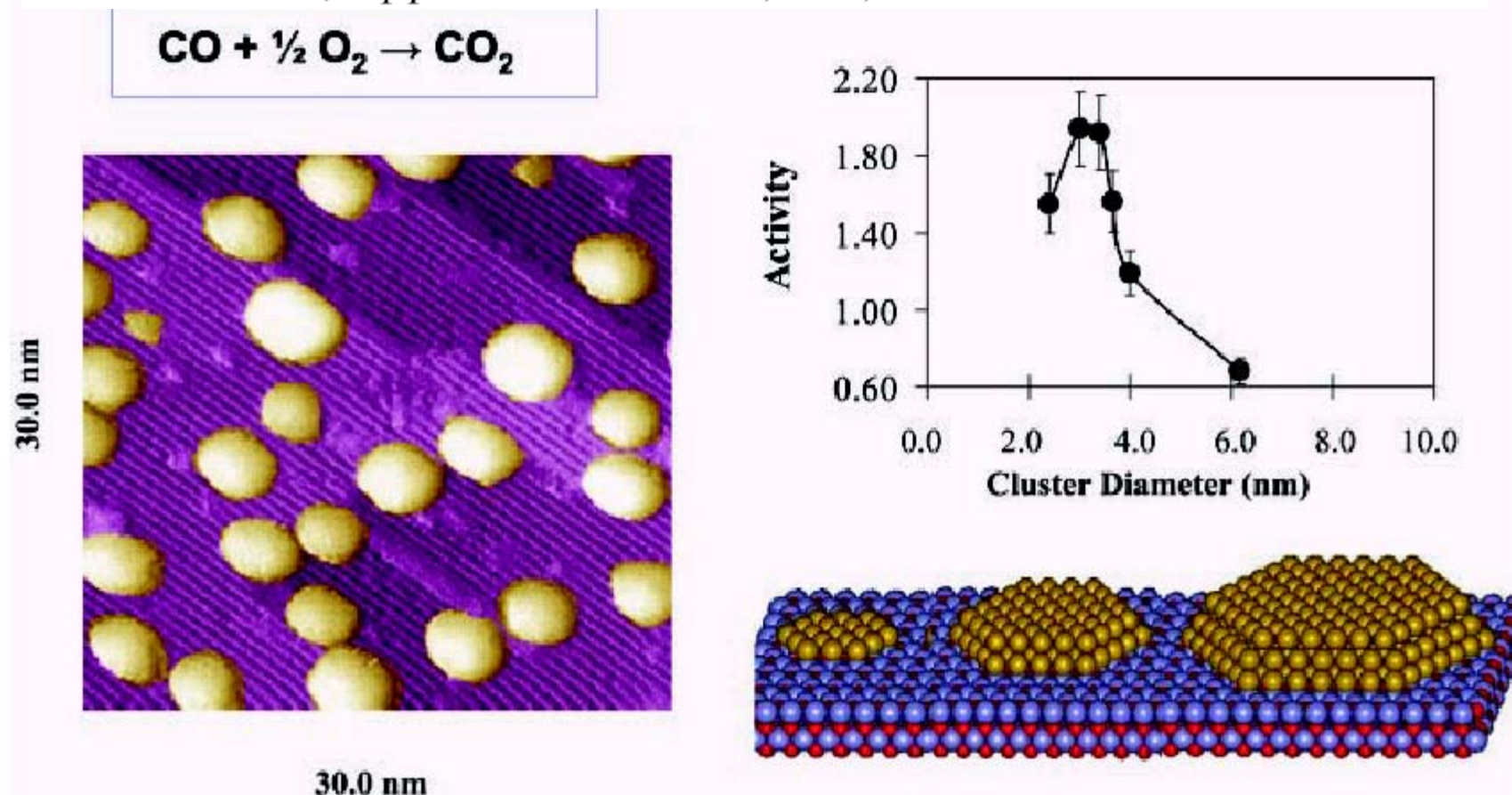


Fig. 2. Effects of particle size on the activity of titania-supported Au for the oxidation of CO (5).

Historical background

- In 1857, Faraday reported the formation of deep red solutions of colloidal gold by reduction of an aqueous solution of chloroaurate (AuCl_4^-) using phosphorus in CS_2 (a two-phase system).
- The most popular method for a long time has been that using citrate reduction of HAuCl_4 in water, which was introduced by Turkevitch in 1951.
- Schmid: Au_{55} cluster (1.4 nm) synthesis
- Brust: Two phase synthesis of Au nanoparticles
- Mirkin: Biosensor applications

The Lycurgus Cup 4th century, Late Roman



green in reflected light;



ruby red in transmitted light

http://www.britishmuseum.org/explore/highlights/highlight_objects/pe_mla/t/the_lycurgus_cup.aspx

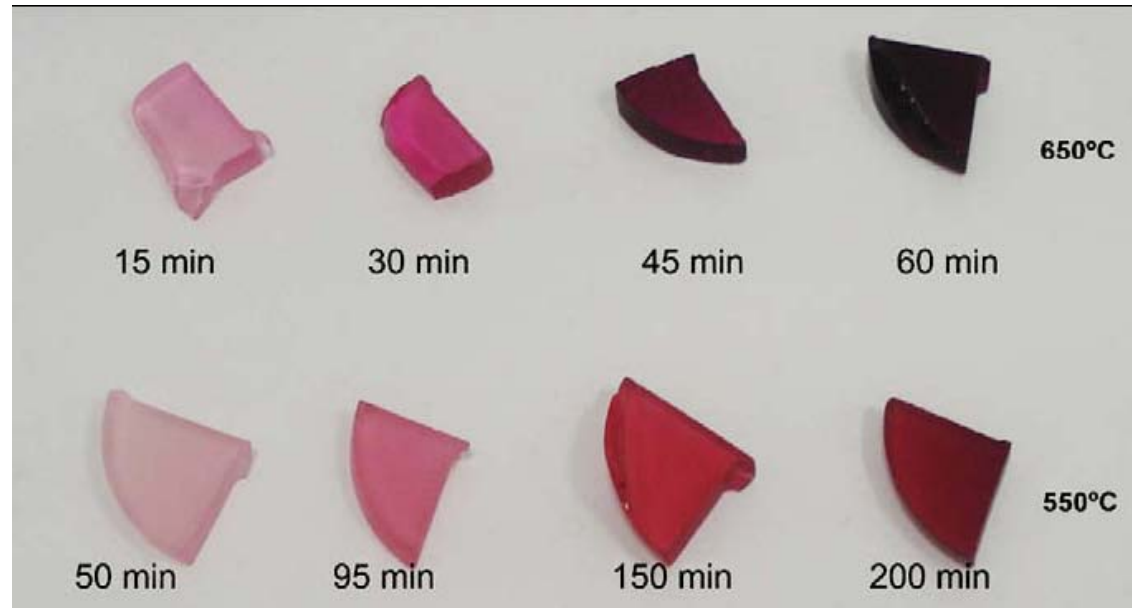
Gold nanoparticles in ancient and contemporary ruby glass,
Andreia Ruivo, et al., *Journal of Cultural Heritage* 9 (2008) e134-e137.

Gold ruby glass was made by irradiating a soda-lime-silicate glass with ca. 0.2 weight % of gold with gamma rays and further heating instead of using a reducing agent such as stannous oxide.



Red-purple glass vase, 17th century,
Monastery of Santa Clara-a-Velha,
Coimbra.

Different colours were obtained by
controlling the temperature and heating times.



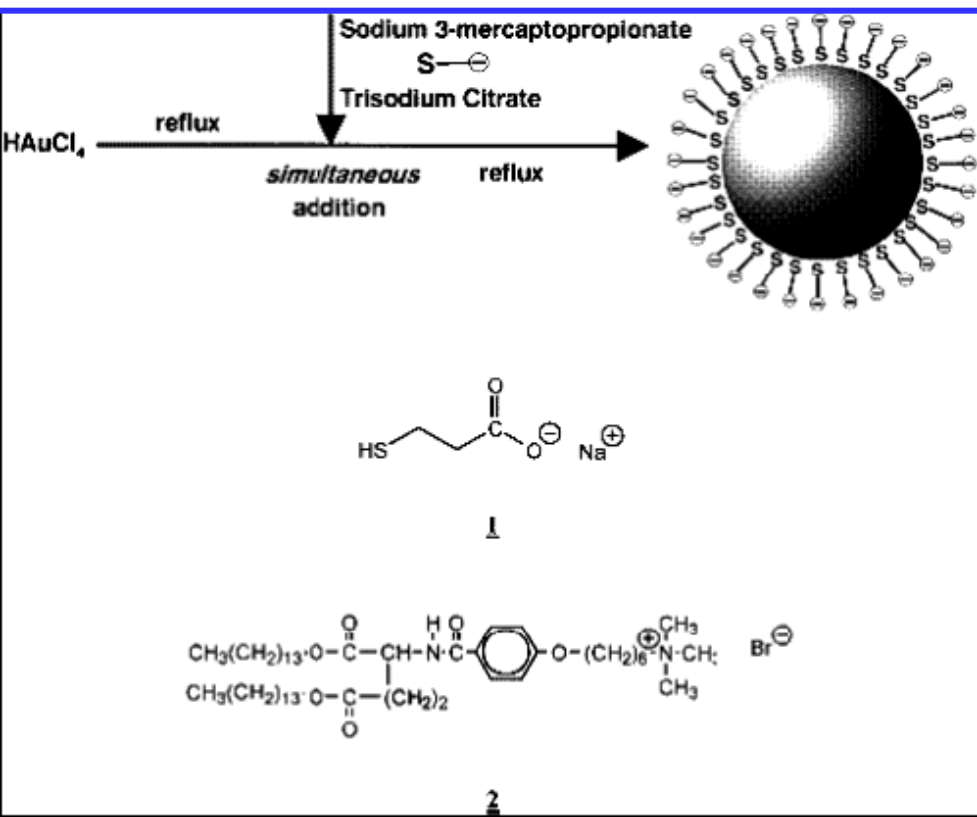
Soda-lime-silicate glass heated at 550 C
and 650 C during different times.

Au clusters

- The pioneering work by Schmid and co-workers on well-defined phosphine-stabilized gold clusters
- The number of atoms in these gold clusters is based on the dense packing of atoms taken as spheres, each atom being surrounded by 12 nearest neighbors. Thus, the smallest cluster contains 13 atoms, and the following layers contain $10n^2 + 2$ atoms, n being the layer number.
- For instance, the second layer contains 42 atoms, which leads to a total of 55 atoms for a gold cluster, and the compound $[\text{Au}_{55}(\text{PPh}_3)_{12}\text{Cl}_6]$ has been well characterized by Schmid's group.
- Recently, spectroscopic data have revealed discrete energy level spacings of 170 meV that can be attributed to the Au_{55} core.
- Larger clusters containing, respectively, 147, 309, 561, 923, 1415, or 2057 ($n = 3\sim 8$) atoms have been isolated.

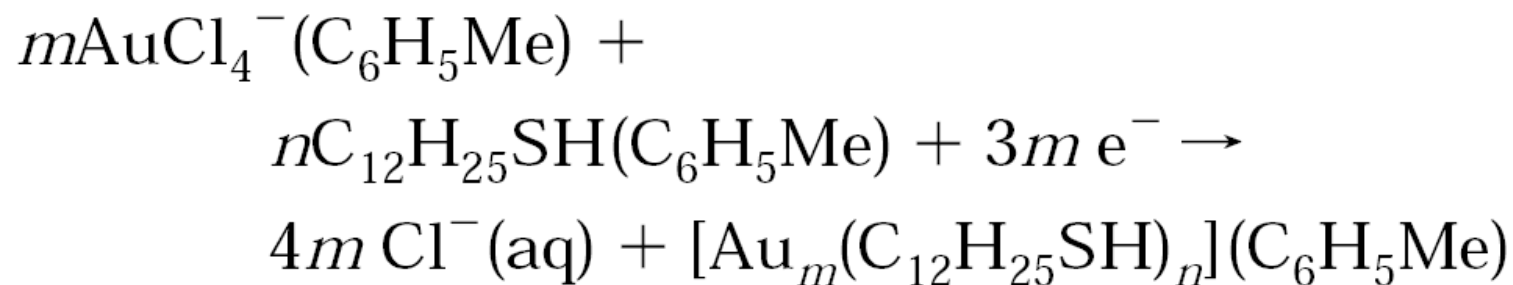
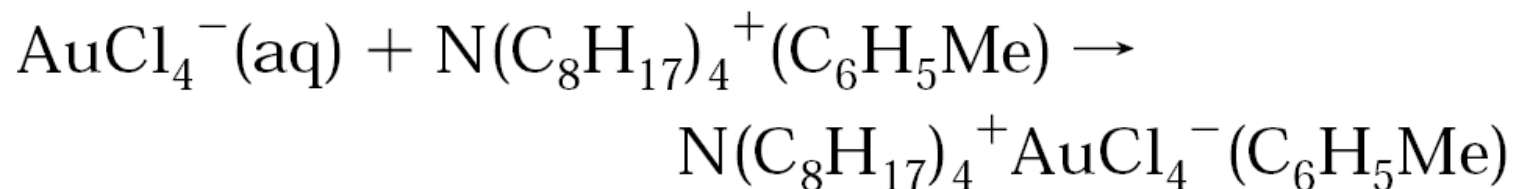
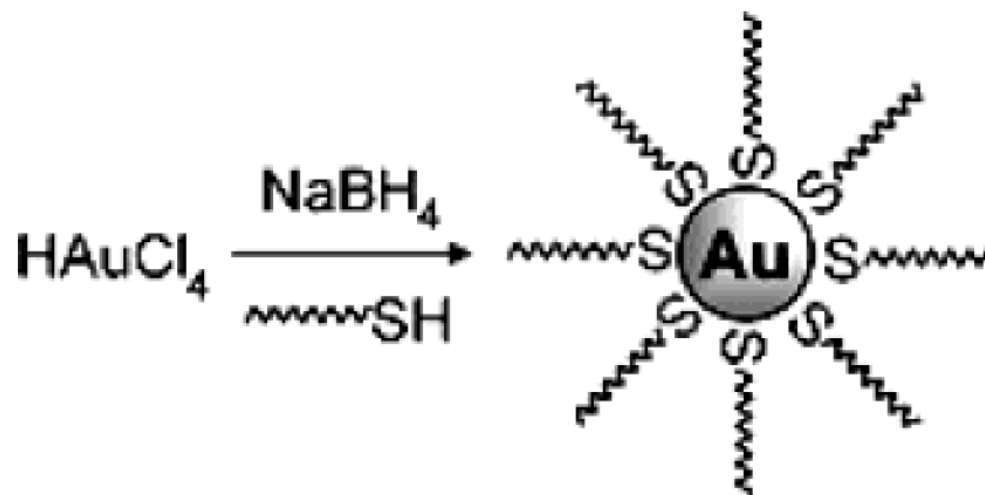
- The stabilization of AuNPs with alkanethiols was first reported in 1993 by Mulvaney and Giersig, who showed the possibility of using thiols of different chain lengths.

Giersig, M.; Mulvaney, P. Preparation of ordered colloid monolayers by electrophoretic deposition. *Langmuir* **1993**, 9, 3408



Synthesis of Thiol-Derivatized Gold Nanoparticles in a Two-phase Liquid-Liquid System.

Brust, M. *J. Chem. Soc., Chem. Commun.* **1994**, 801-802.



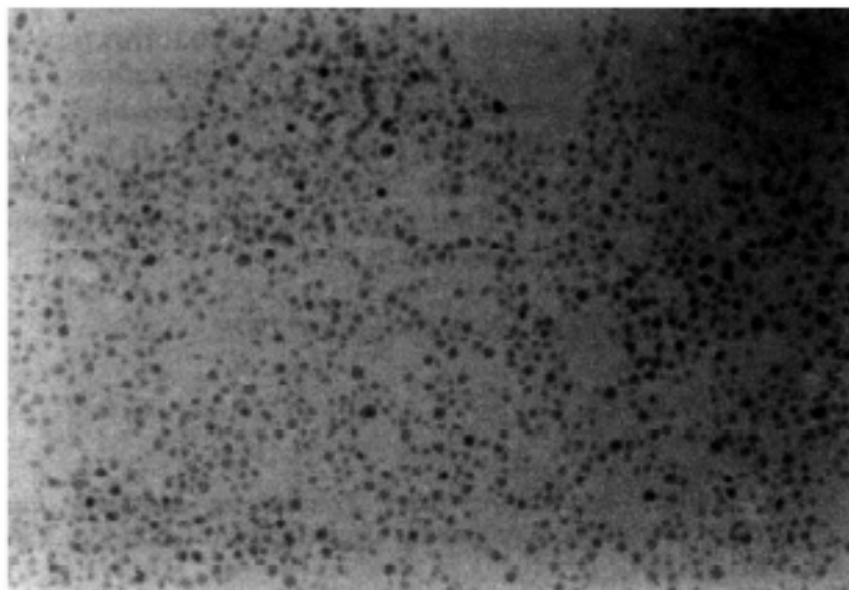
**Title: SYNTHESIS OF THIOL-DERIVATIZED GOLD
NANOPARTICLES IN A 2-PHASE LIQUID-LIQUID SYSTEM**

Author(s): BRUST, M; WALKER, M; BETHELL, D, et al.

**Source: JOURNAL OF THE CHEMICAL SOCIETY-CHEMICAL
COMMUNICATIONS Issue: 7 Pages: 801-802 Published: APR
7 1994**

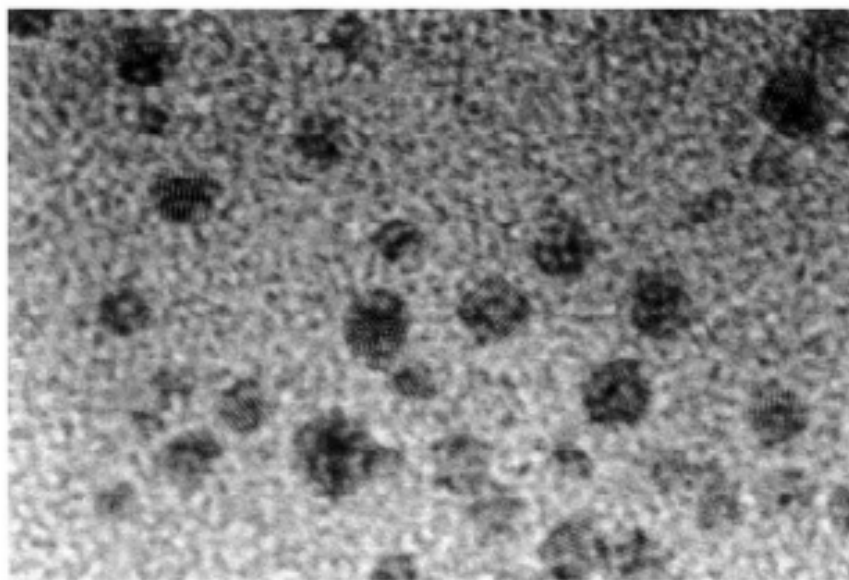
Times Cited: 2,746

- Brust reported a so-called two-phase (or biphasic) method for synthesizing relatively uniform-sized 1-3 nm gold nanoparticles from the reduction of a gold salt in a toluene solution.
- In this process, Hydrogen tetrachloroaurate ($\text{HAuCl}_4 \cdot 3\text{H}_2\text{O}$) dissolved in water was transferred into a toluene solution containing alkanethiol using tetraoctylammonium bromide (TOAB, $(\text{octyl})_4\text{N}^+\text{Br}^-$) as a phase transfer reagent.
- The subsequent reduction was performed by adding NaBH_4 to the toluene solution with vigorous stirring. This biphasic method has been used extensively for synthesizing gold nanoparticles as well as nanoparticles of other noble metals.



30 nm

(b)



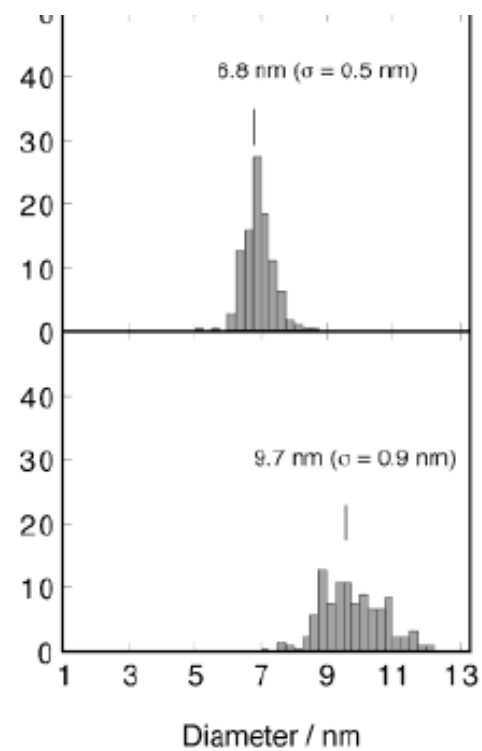
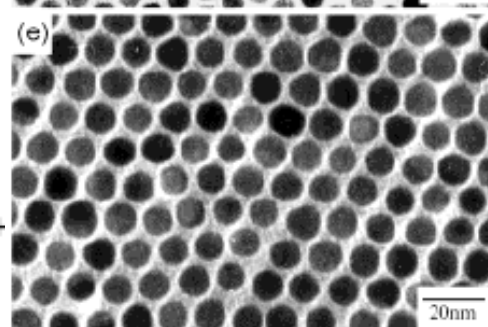
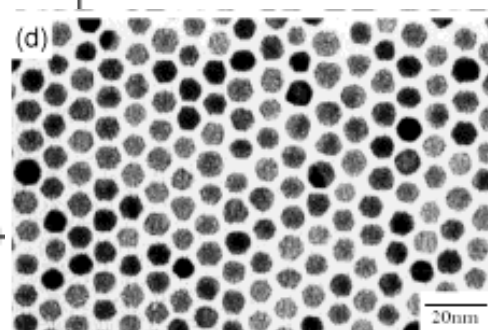
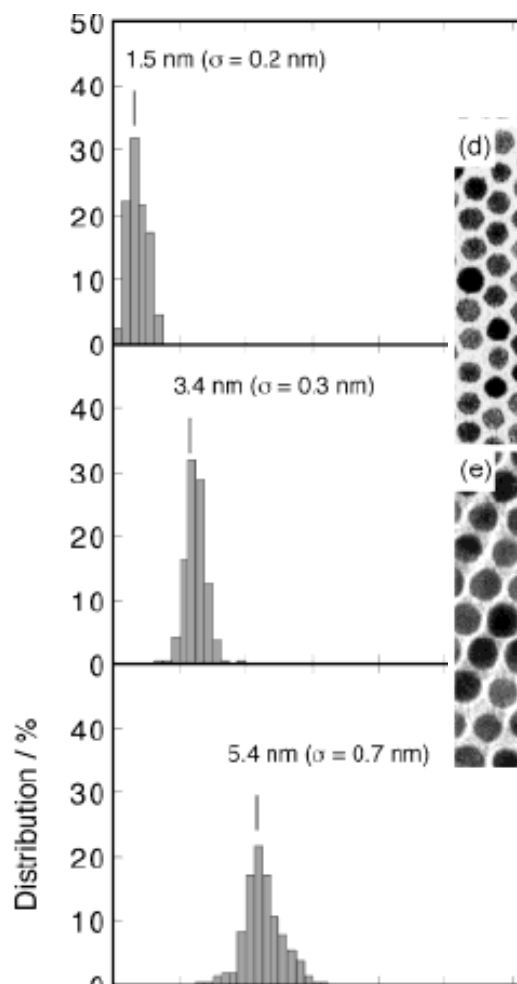
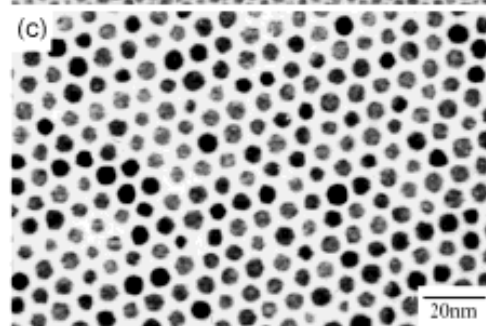
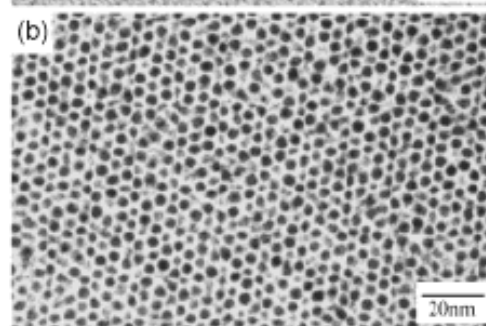
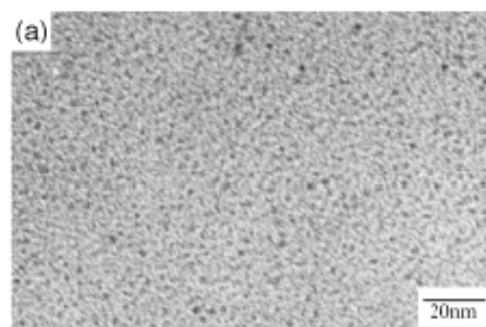
5 nm

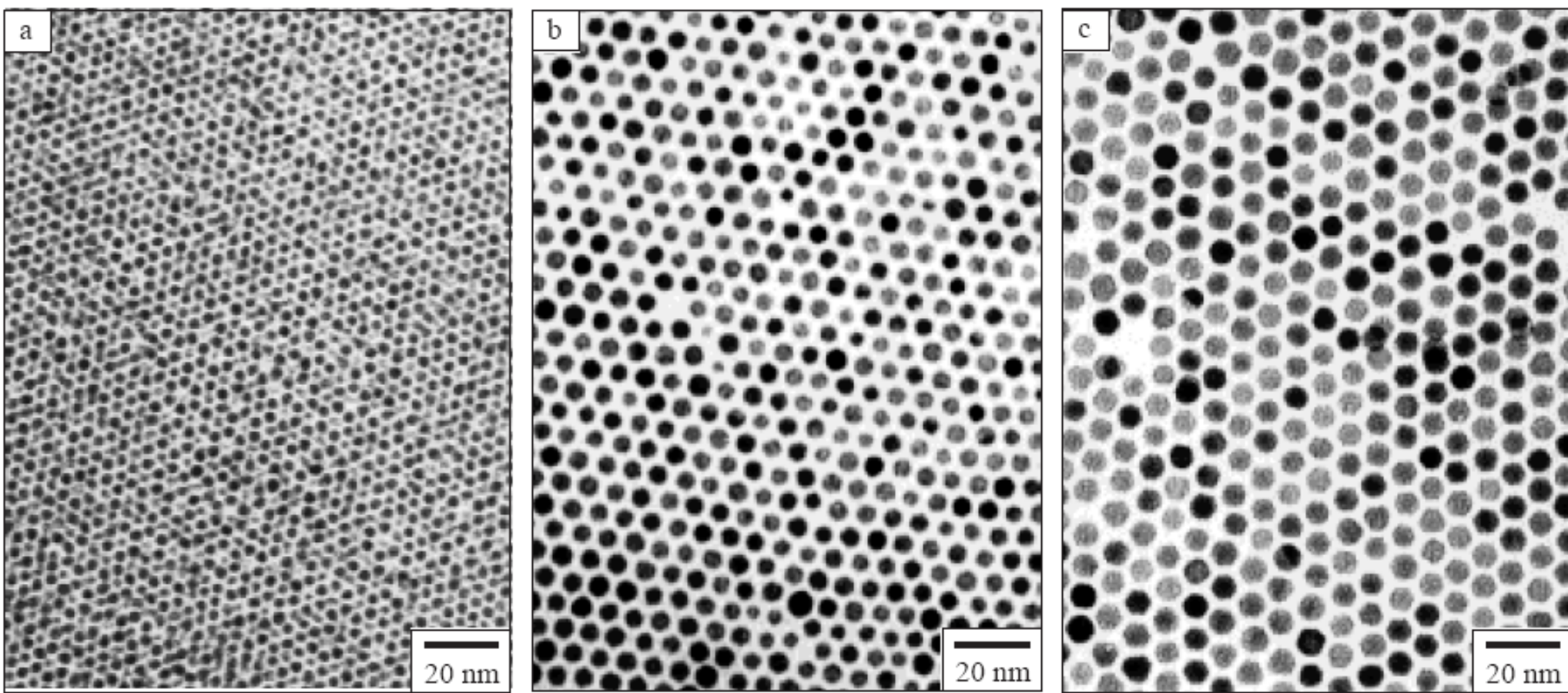
Size Evolution of Alkanethiol-Protected Gold Nanoparticles by Heat Treatment in Solid state

Teranishi, and Miyake, *J. Phys. Chem. B* **2003**, *107*, 2719

See also *Adv. Mater.* **2001**, *13*, 1699.

- The initial dodecanethiol-stabilized 1.5 nm sized gold nanoparticles, which were prepared by Brust's two-phase method,
- Increased in size to 3.4, 5.4, and 6.8 nm by heating at 150, 190, and 230 °C, respectively.
- Thermolysis of crude preparations of Brust's AuNPs without removing the phase-transfer reagent, tetraoctylammonium bromide, to 150-25 °C led to an increase of the particle sizes to 3.4-9.7 nm.



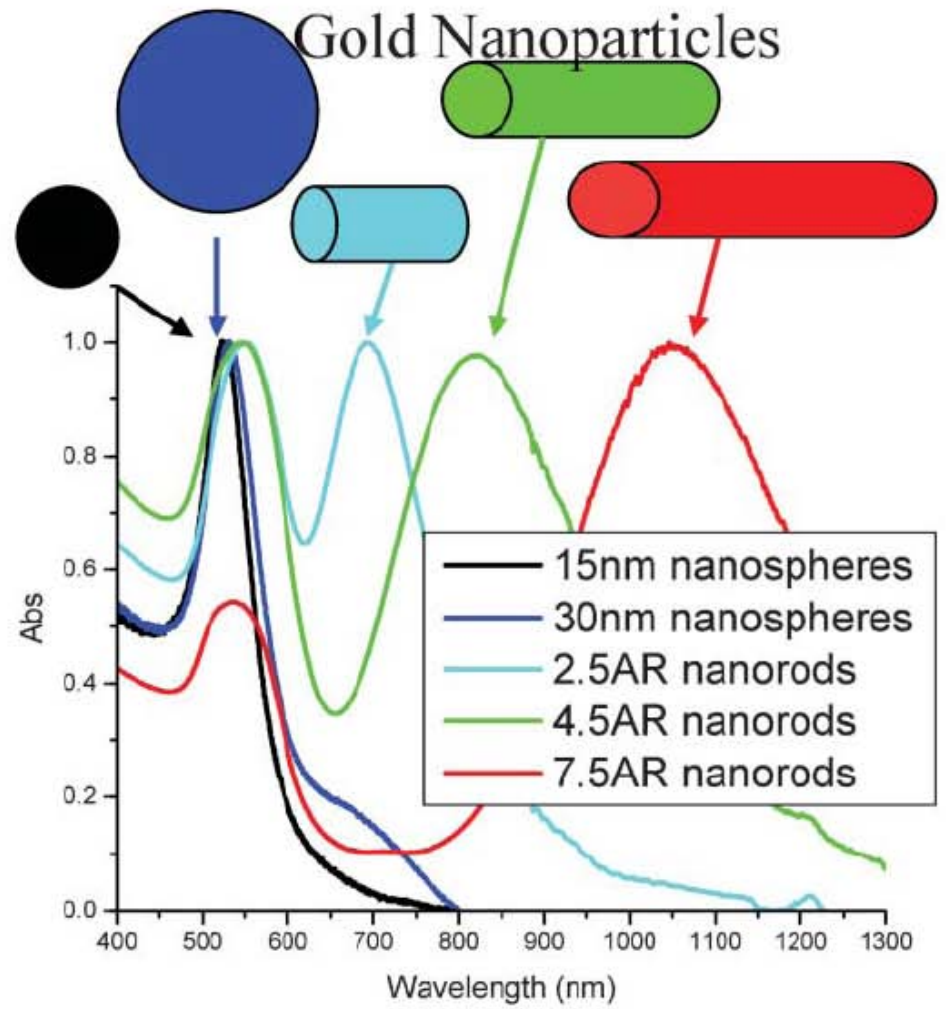
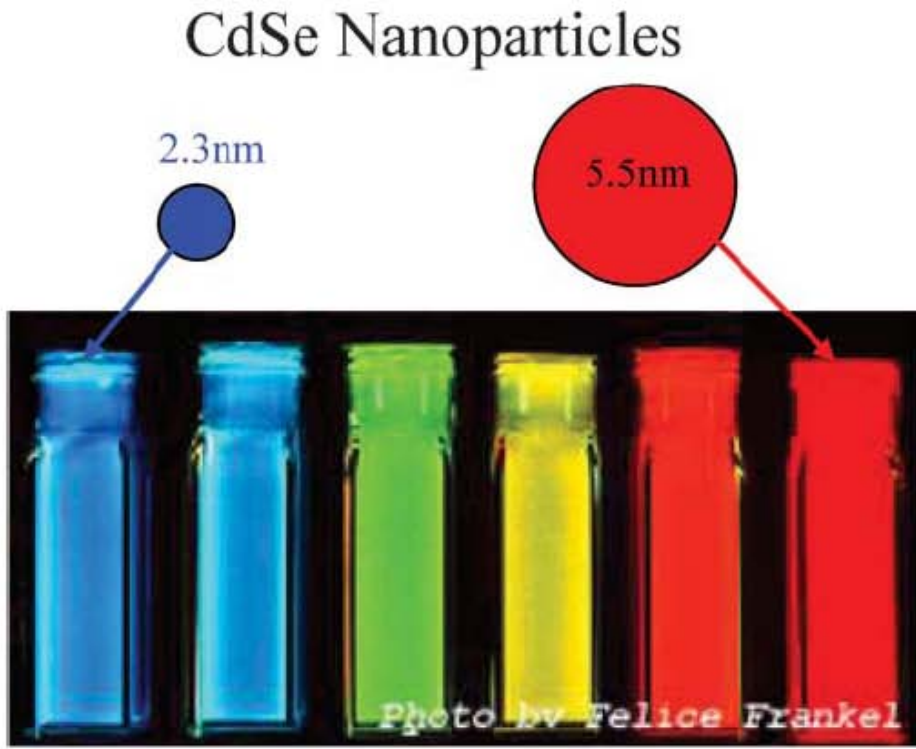


Temp. [°C]	MD [nm]	SD [nm]	[Au] [wt.-%]
—	1.5	0.2	71.9
150	3.4	0.3	79.7
190	5.4	0.7	93.3
230	6.8	0.5	94.7

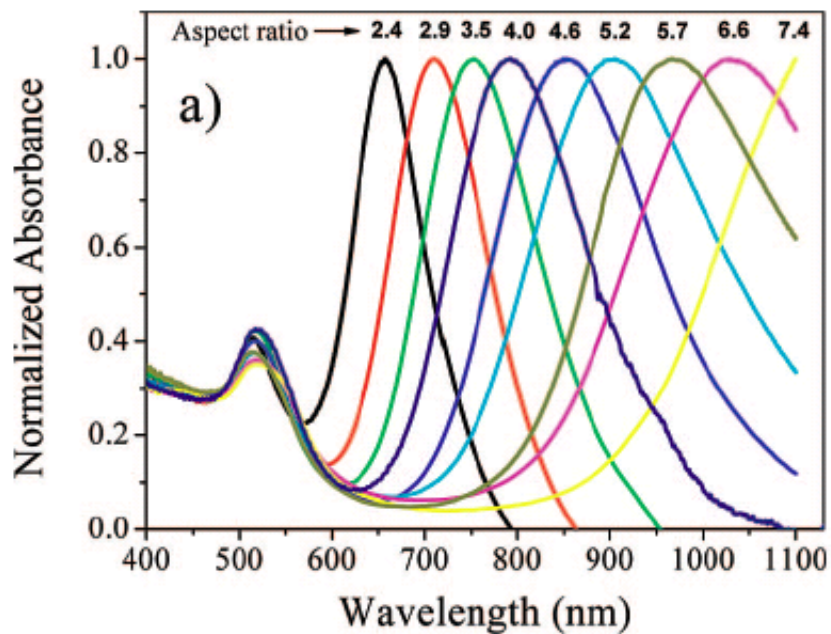
Adv. Mater. **2001**,
13, 1699.

QD's vs. Metal Nanoparticles

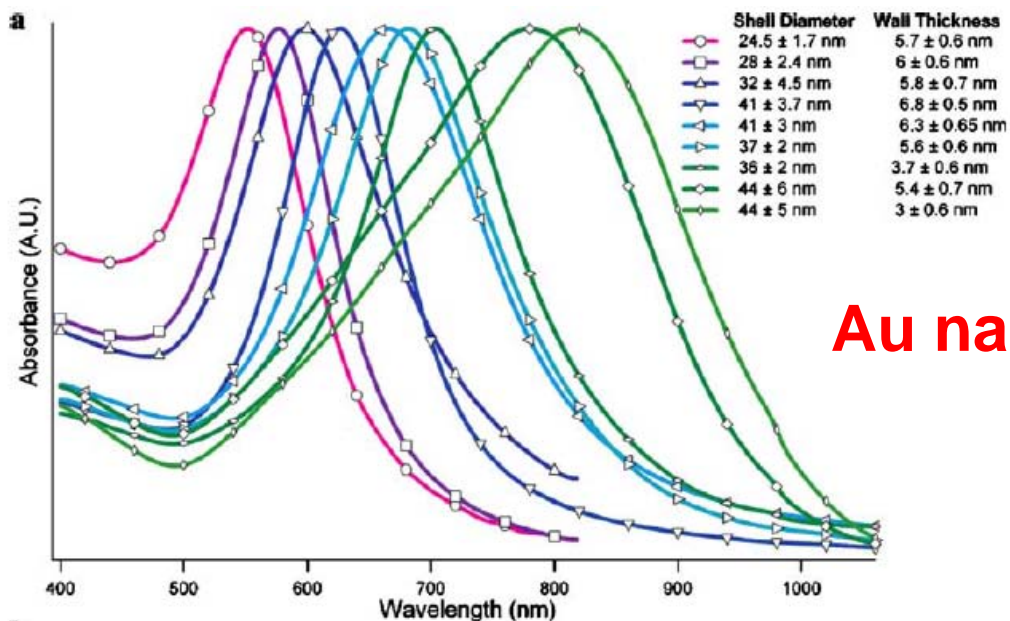
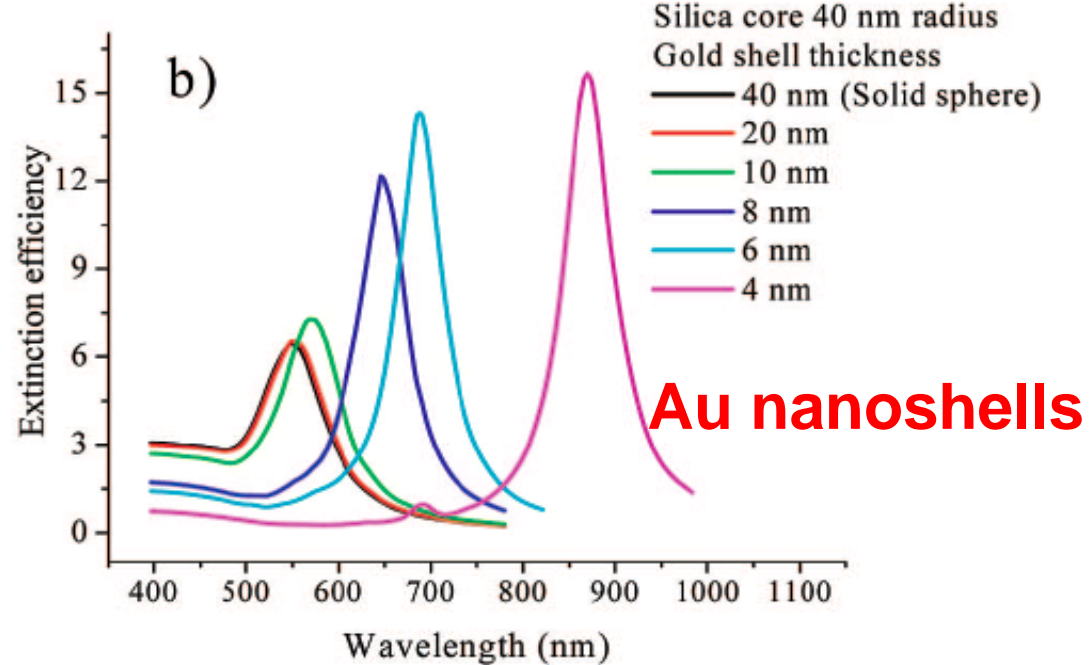
- This absorption does not derive from transitions between quantized energy states.
- Instead, in metal particles, collective modes of motion of the electron gas can be excited. They are referred to as **surface plasmons**.
- Freely mobile electrons are trapped in such metal boxes and show a characteristic collective oscillation frequency of the plasma resonance, giving rise to the so-called plasmon resonance band (PRB) observed near 530 nm in the 5-20-nm-diameter range.
- The **size dependence** of the plasmon frequency is **negligible**: No shift in Absorption maximum for colloidal gold nanocrystals in the range between 5 and 30 nm.



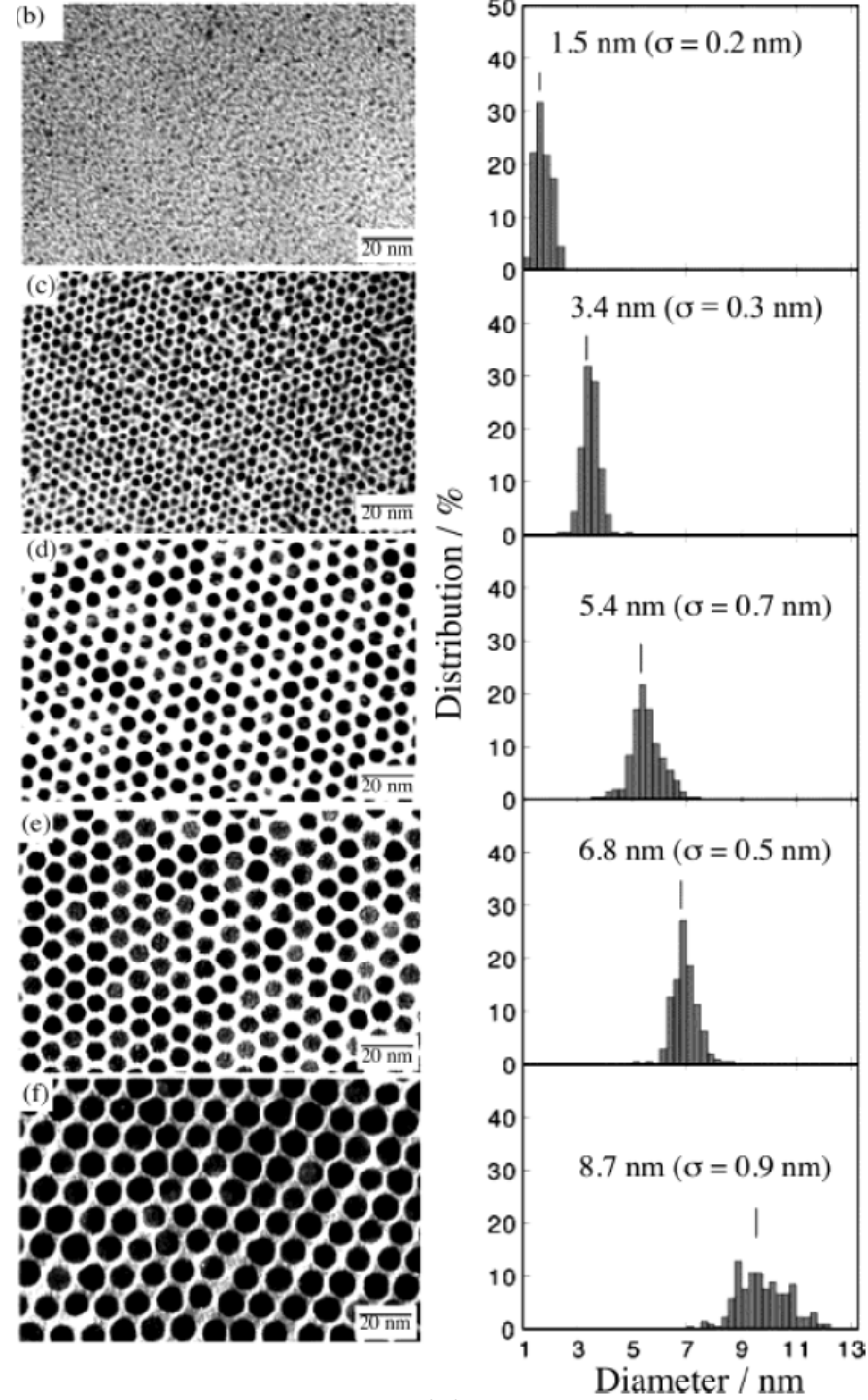
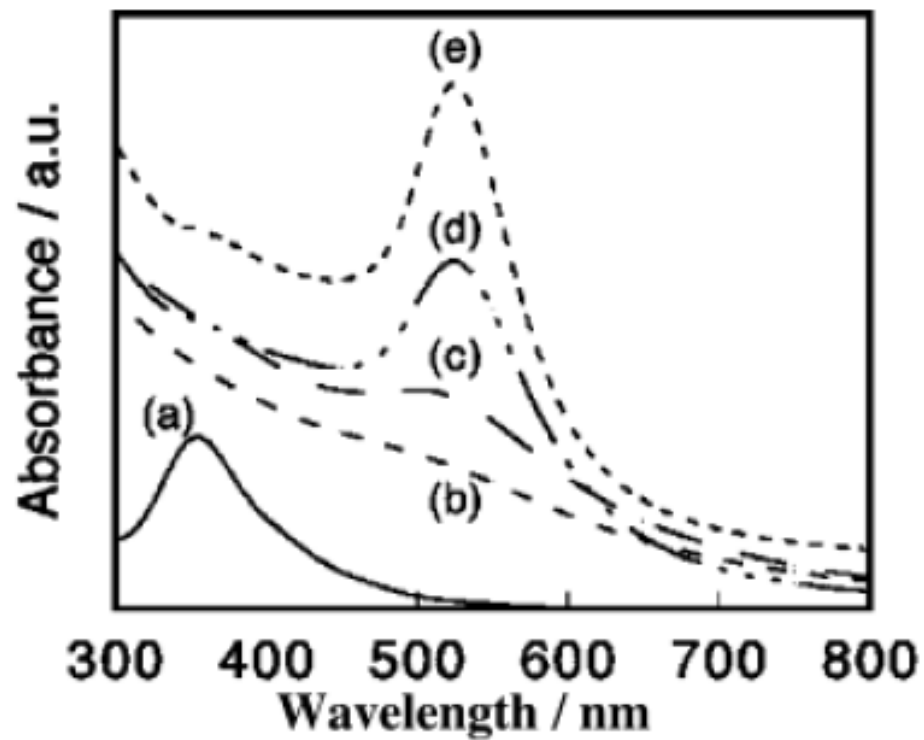
S. Eustis, M. A. El-Sayed, *Chem. Soc. Rev.* **2006**, 35, 209-217.



Au nanorods



Au nanoshells

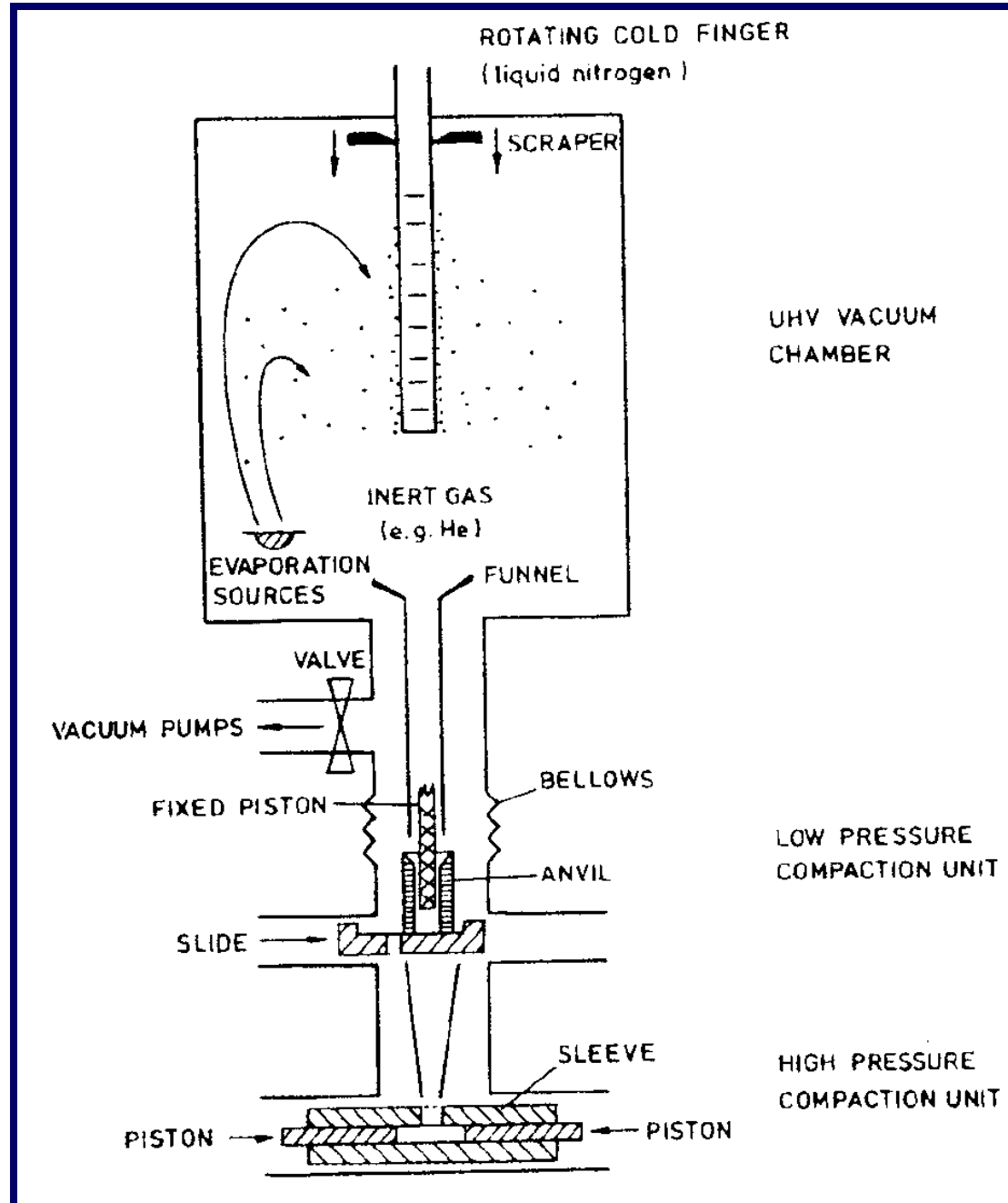


**Gram-Scale Synthesis of Monodisperse Gold Colloids by the
Solvated Metal Atom Dispersion Method and Digestive
Ripening and Their Organization into Two- and
Three-Dimensional Structures**

Kenneth J. Klabunde (Kansas State University)

JACS 2002, 124, 2305

Vapor Condensation Method



Gleiter, H.
Adv. Mater. **1992**, 4, 474

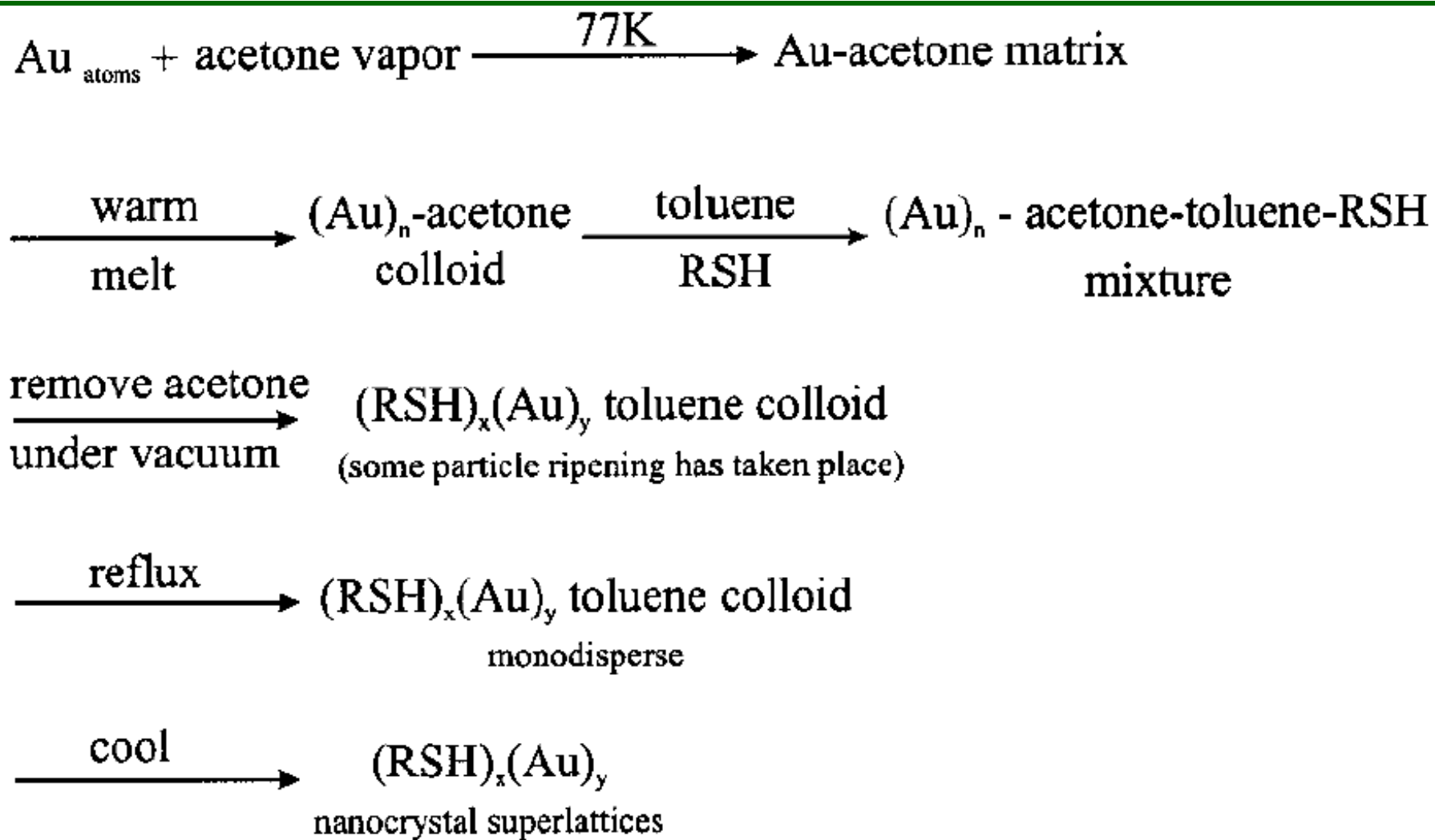
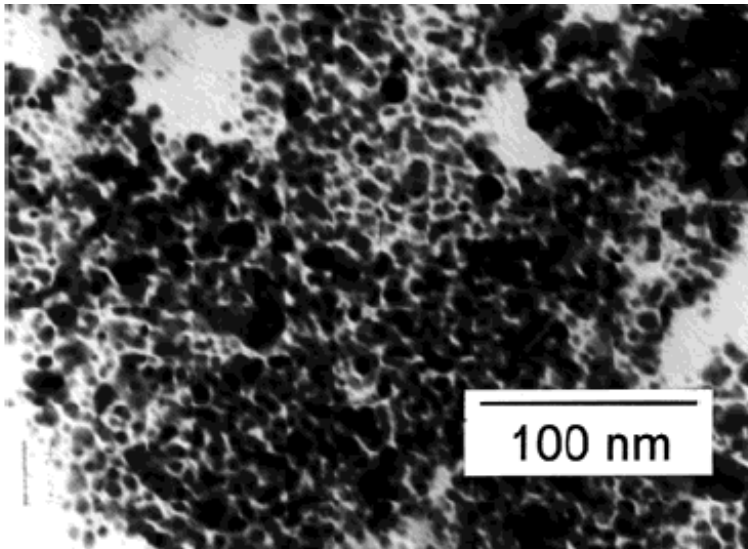
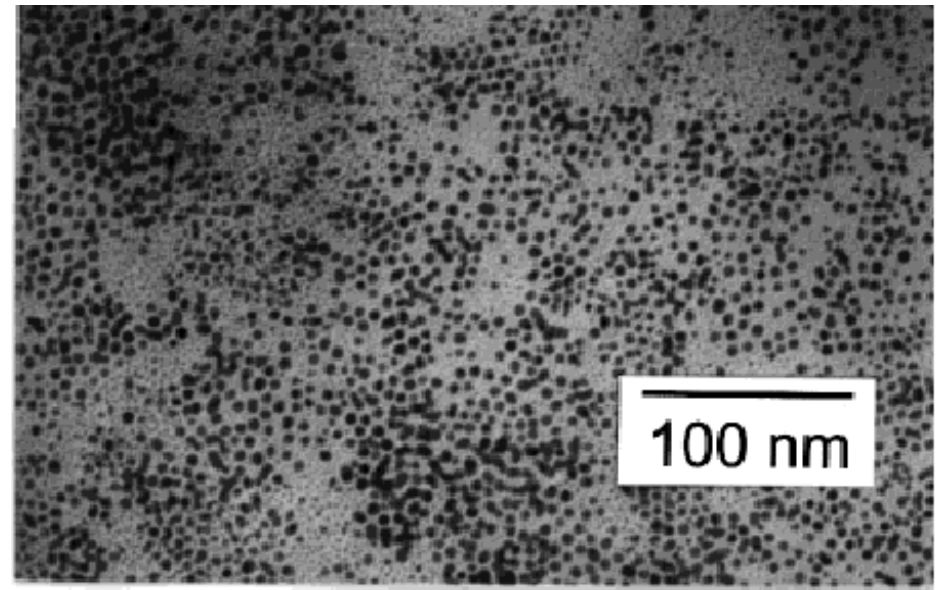
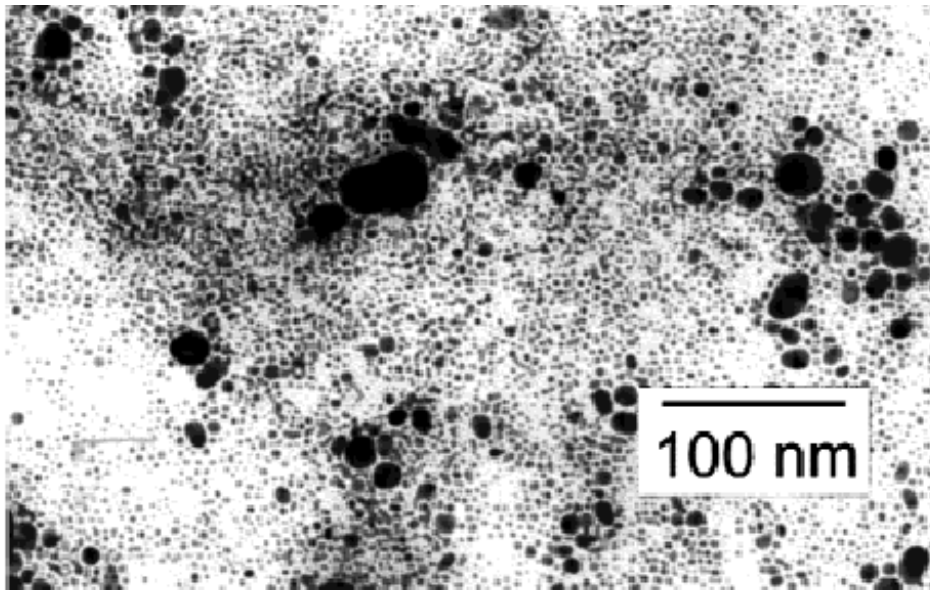


Figure 1. Flow diagram of synthetic steps for preparation of nanocrystal superlattices.

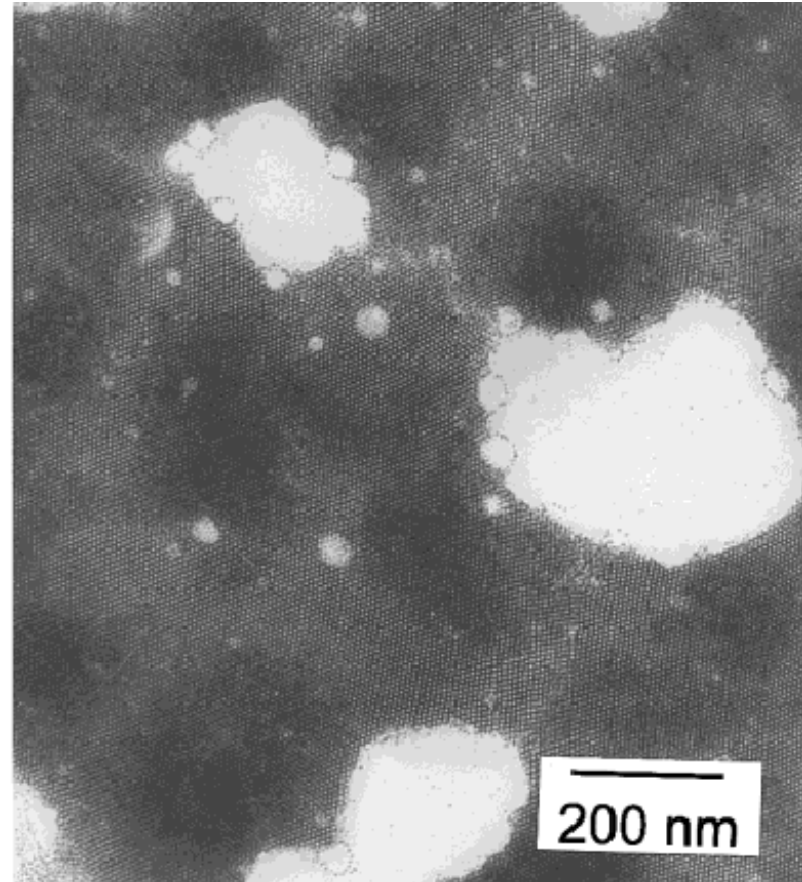
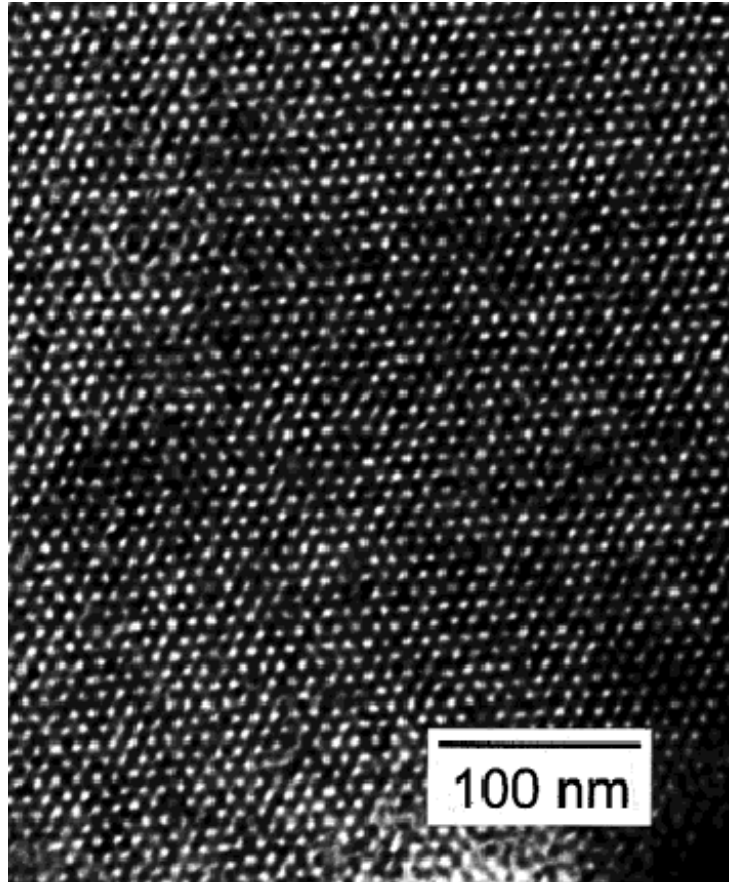


Au-acetone-toluene-thiol colloid
Initial NP: 5 ~ 40 nm
polydisperse

Figure 2. TEM micrograph of gold particles from Au-acetone-toluene-thiol colloid (colloid 1).



Au-toluene-thiol colloid



1 day digestive ripening process; 3 month

Long-range ordered Nanocrystal Superlattices on SiN

JPC-B 2001, 105, 3353 by Klabunde at Kansas SU.

Synthesis of Monodisperse Au Nanoparticles

Reduction of AuCl_3 using NaBH_4 in the presence of DDAB (didodecyldimethylammonium bromide)

Ligand exchange with dodecanethiol

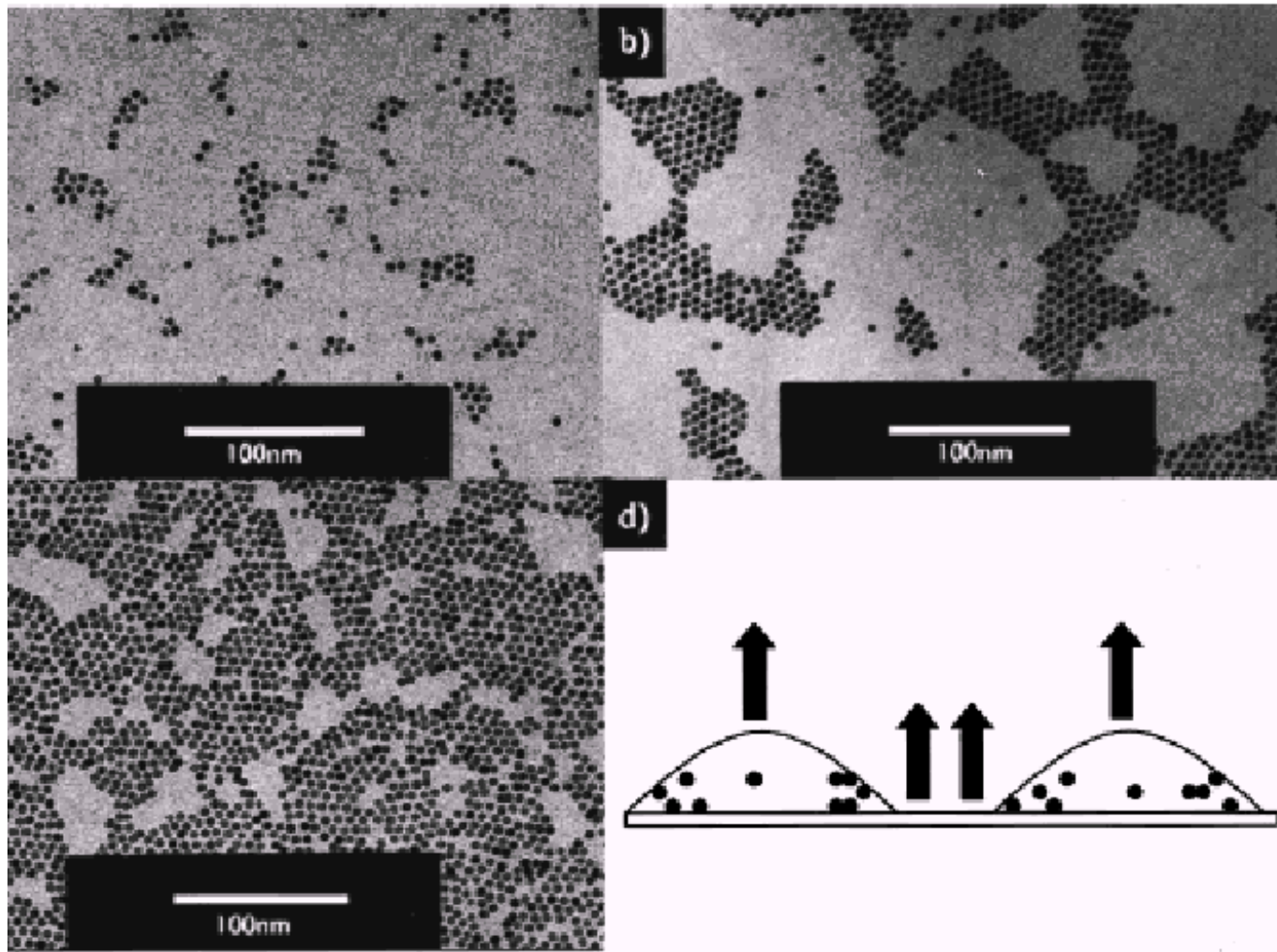
Refluxing in toluene narrows the size distribution

Synthesis of 5.5 nm Au NP's with std of 5 %

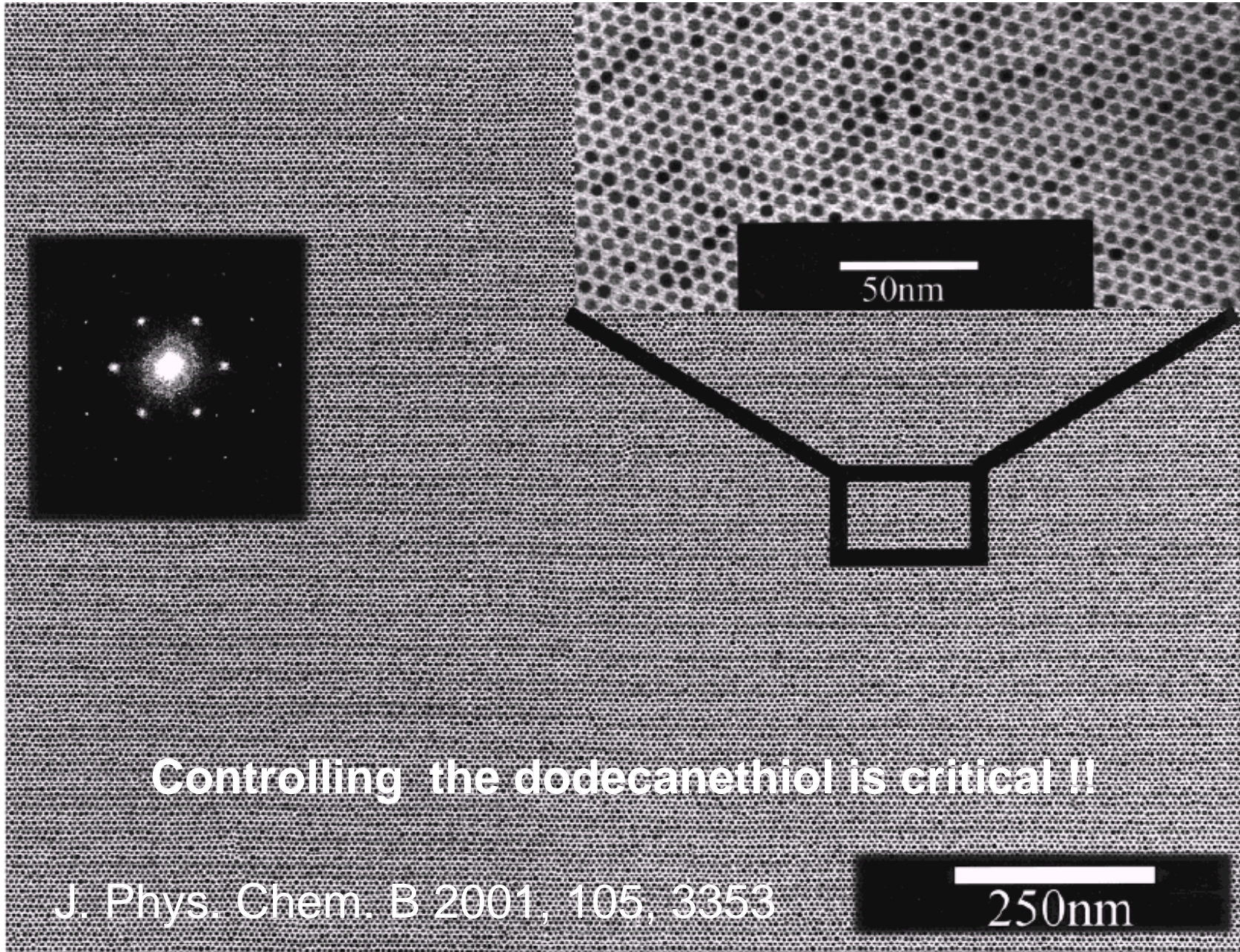
- Evaporation of solvent induces superlattice formation
- So far only few hundreds of nanometers
- Polarity of the solvent affects wetting properties, influencing the aggregation of nanocrystals on the surface (PRL 198, 80, 3531)
- Competition of 2D superlattice formation and solvent dewetting
- Control of dewetting process to get long-range ordered superlattice

With domain size of several microns.

When pure toluene was used, evaporation is too fast to form superlattice.



Superlattice formation in micrometer-scale

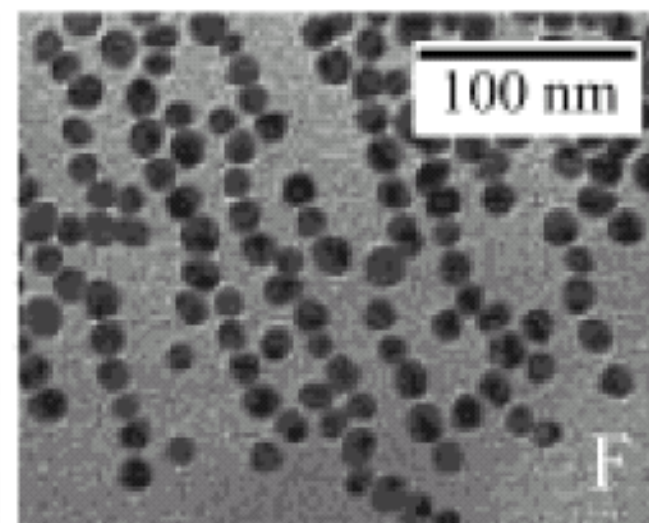
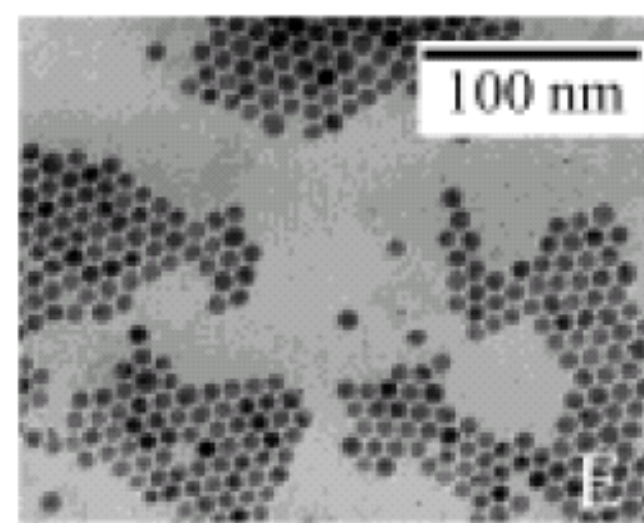
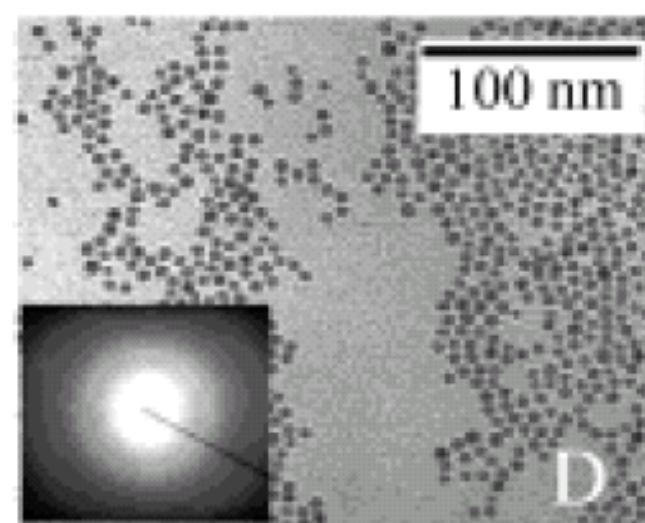
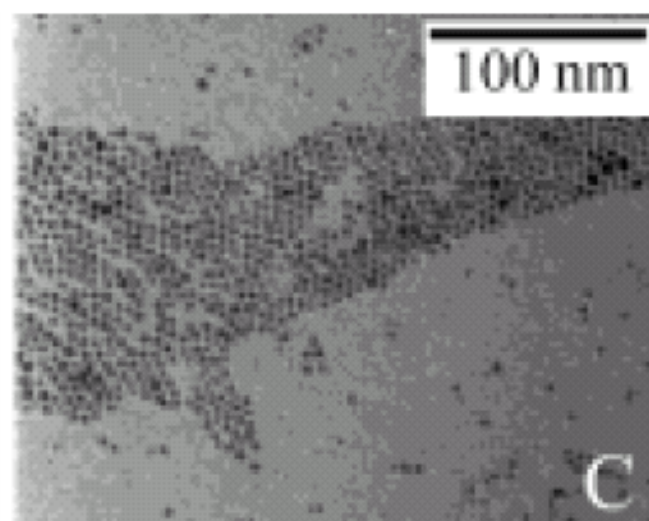
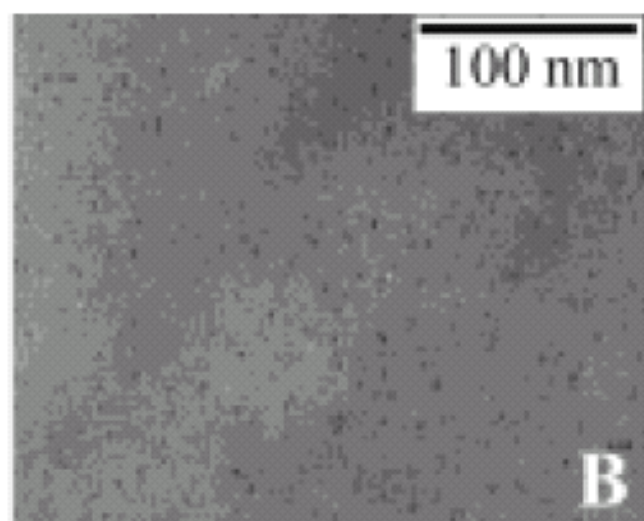
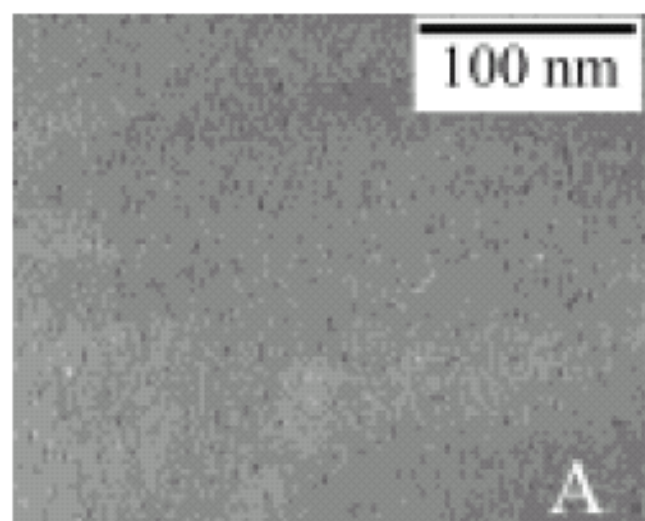


- Control of particle-particle and particle-substrate interaction to self-assemble superlattice structures upon drying
- Rapid dewetting of volatile solvent: bad for superlattice formation
- Long-range superlattice formation through increasing the concentration of nonvolatile dodecanethio ligand.
- Monolayer and bilayer control by NP concentration

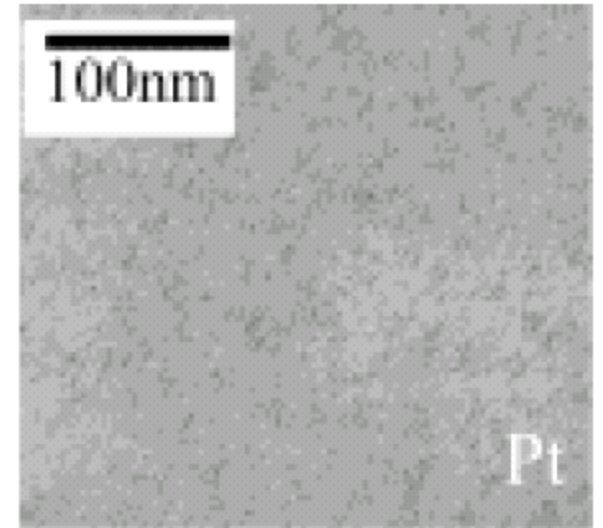
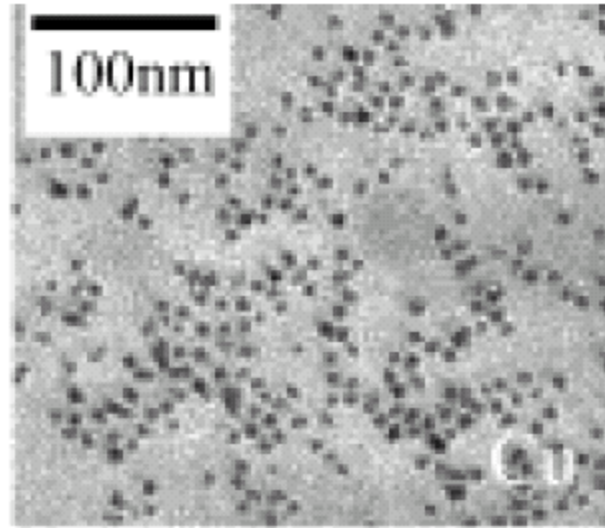
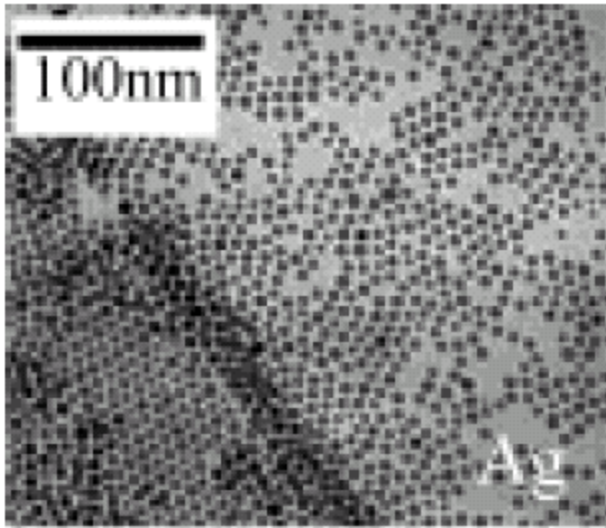
X. G. Peng, *J. AM. CHEM. SOC.* 2003, 125, 14280.

Single-phase system Synthesis

- AuCl_3 , $\text{Ag}(\text{CH}_3\text{COO})$, $\text{Cu}(\text{CH}_3\text{COO})_2$, or PtCl_4 was dissolved in toluene with an ammonium surfactants.
- Either **tetrabutylammonium borohydride (TBAB)** or its mixture with hydrazine in toluene was used as reducing reagents.
- Fatty acids or aliphatic amines were added as ligands.



Ag, Cu, and Pt nanocrystals



Applications of Gold Nanoparticles

See references 506 – 517 of
Chem. Rev. **2004**, 104, 293-346.

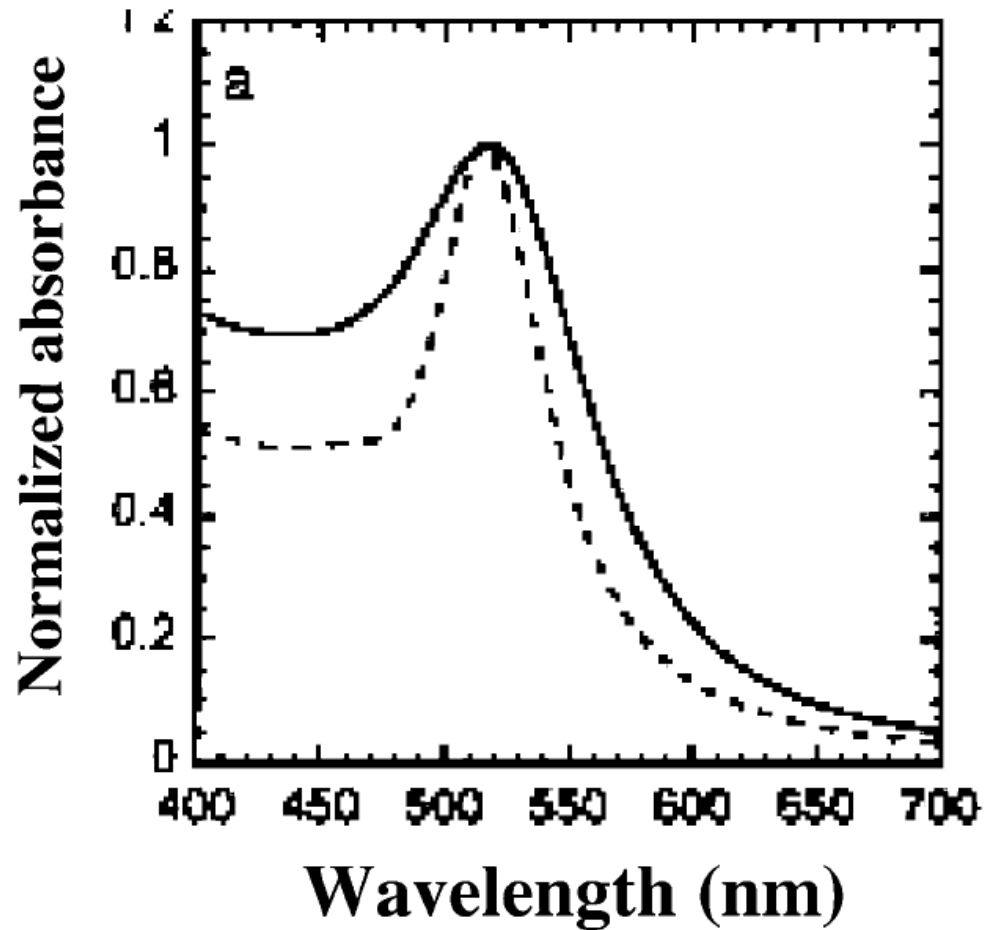
Surface Plasmon Band (SPB)

- Freely mobile electrons are trapped in such metal boxes and show a characteristic collective oscillation frequency of the plasma resonance, giving rise to the so-called plasmon resonance band (PRB) observed near 530 nm in the 5-20-nm-diameter range.
- The deep-red color of AuNP sols in water and glasses reflects the surface plasmon band (SPB), a broad absorption band in the visible region around 520 nm.
- The SPB is due to the collective oscillations of the electron gas at the surface of nanoparticles (6s electrons of the conduction band for AuNPs) that is correlated with the electromagnetic field of the incoming light, i.e., the excitation of the coherent oscillation of the conduction band.

Main characteristics of SPB

- (i) its position around 520 nm;
- (ii) its sharp decrease with decreasing core size for AuNPs with 1.4-3.2-nm core diameters due to the onset of quantum size effects that become important.
- (iii) SPB is absent for AuNPs with core diameter less than 2 nm, as well as for bulk gold.
- (iv) For AuNPs of mean diameter of 9, 15, 22, 48, and 99 nm, the SPB maximum λ_{\max} was observed at 517, 520, 521, 533, and 575 nm, respectively, in aqueous media.
- (v) The SPB maximum and bandwidth are also influenced by the **particle shape**, medium dielectric constant, and temperature.

Optical absorption spectra of 8.3 nm Au nanoparticles in water



Programmed Materials Synthesis with DNA

James J. Storhoff and Chad A. Mirkin*

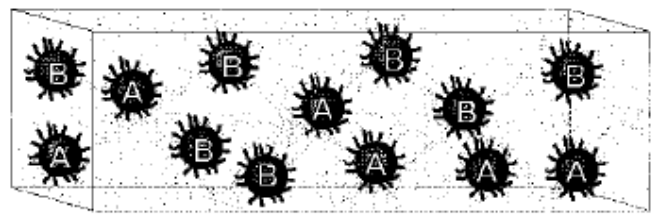
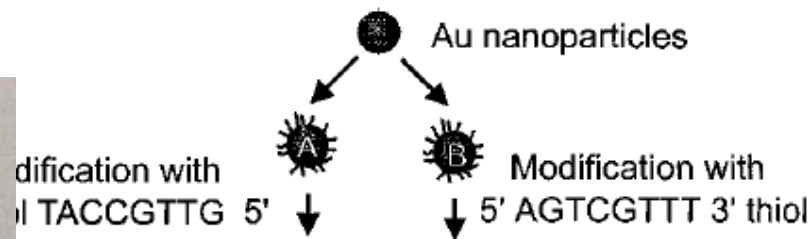
Chem. Rev. **1999**, 99, 1849-1862

ORIGINAL PAPER:

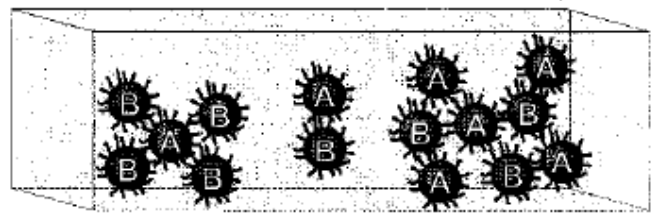
DNA Based Method for Rationally Assembling Nanoparticles
Into Macroscopic Materials.

Mirkin, C. A.; Letsinger, R. L.; Mucic, R. C.; Storhoff, J. J.

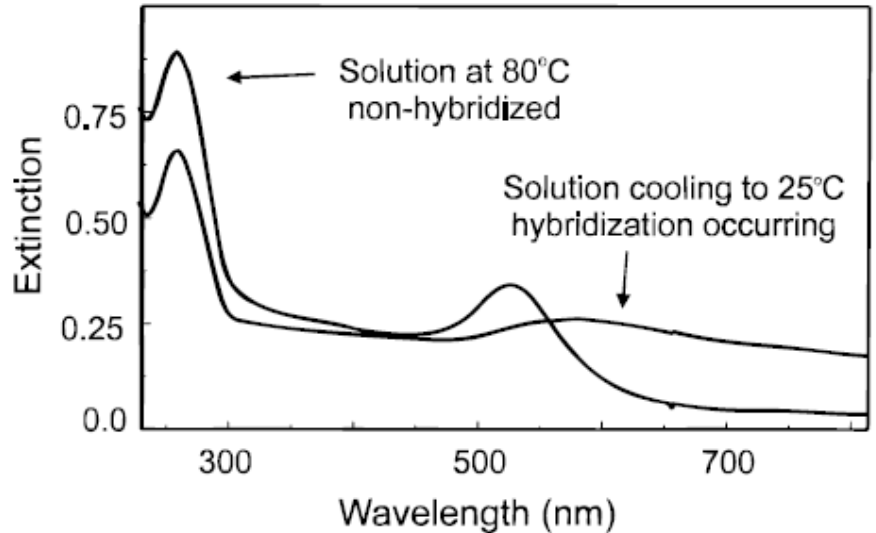
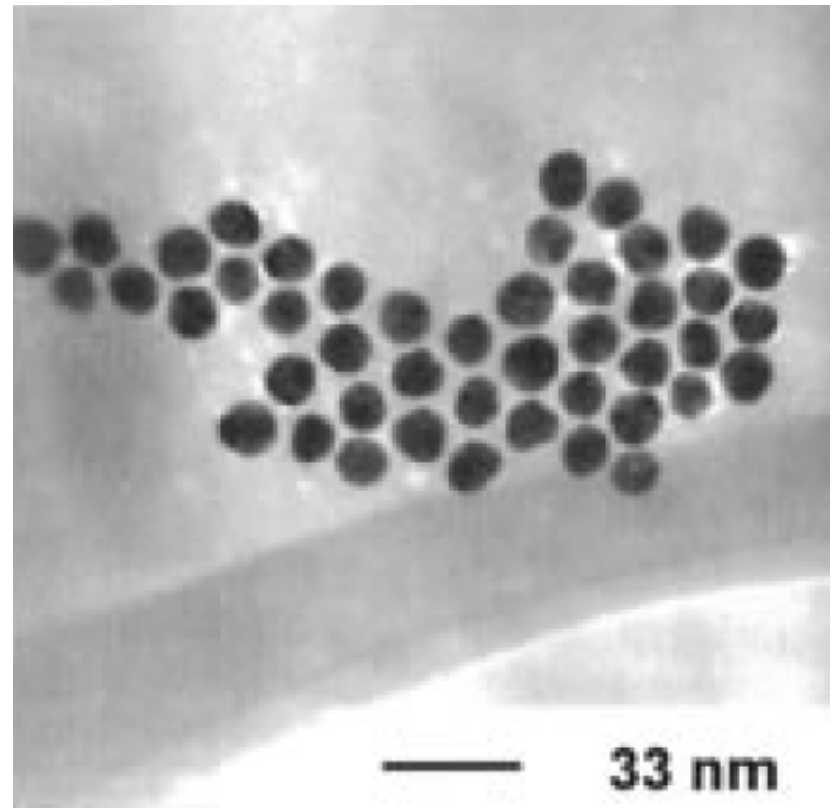
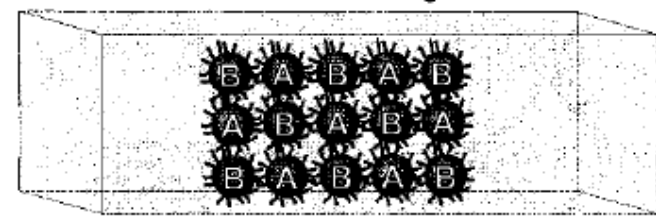
Nature **1996**, 382, 607-609.



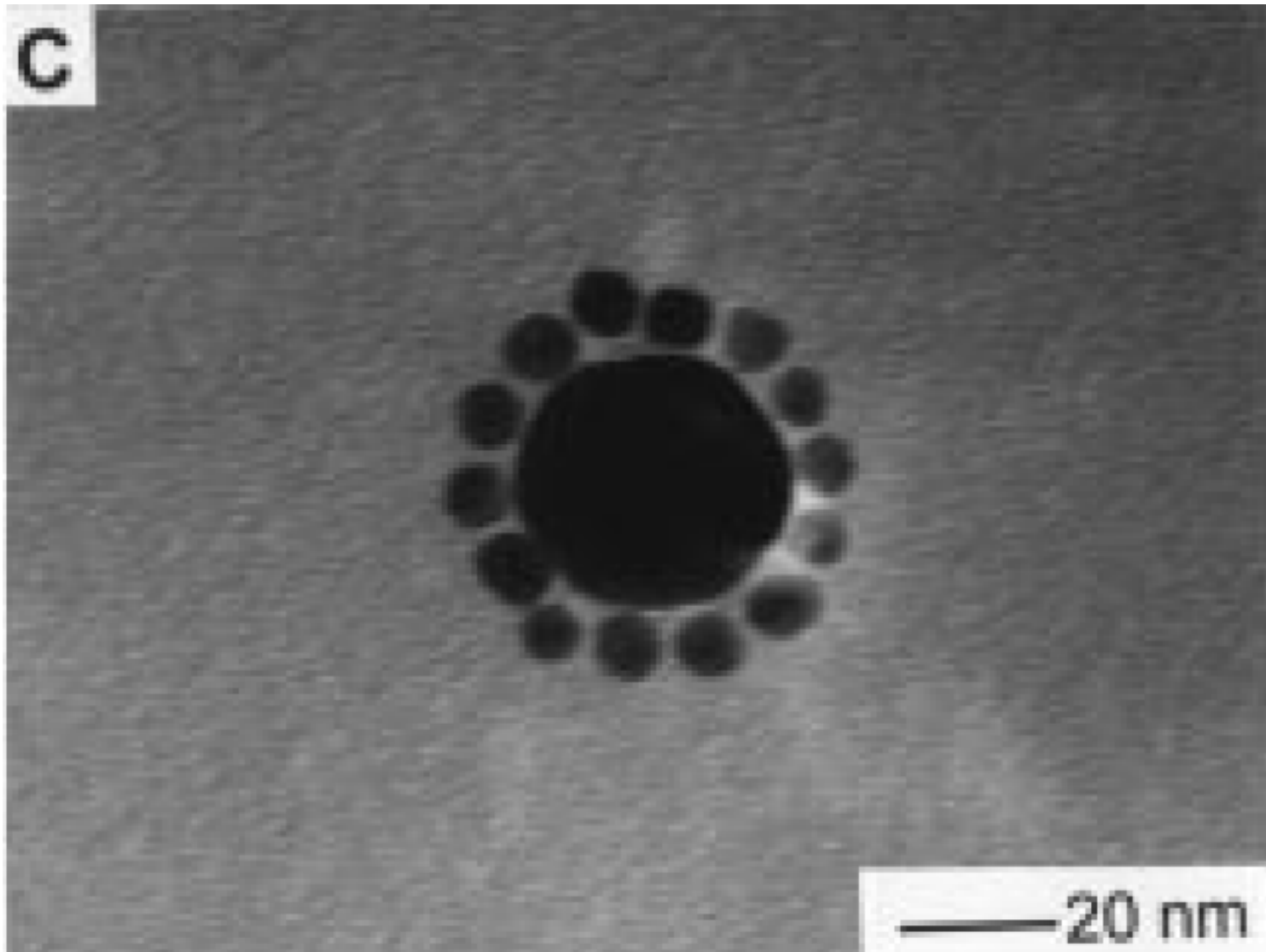
Δ↑↓ Addition of linking DNA duplex
5' ATGGCAAC  TCAGCAA 5'

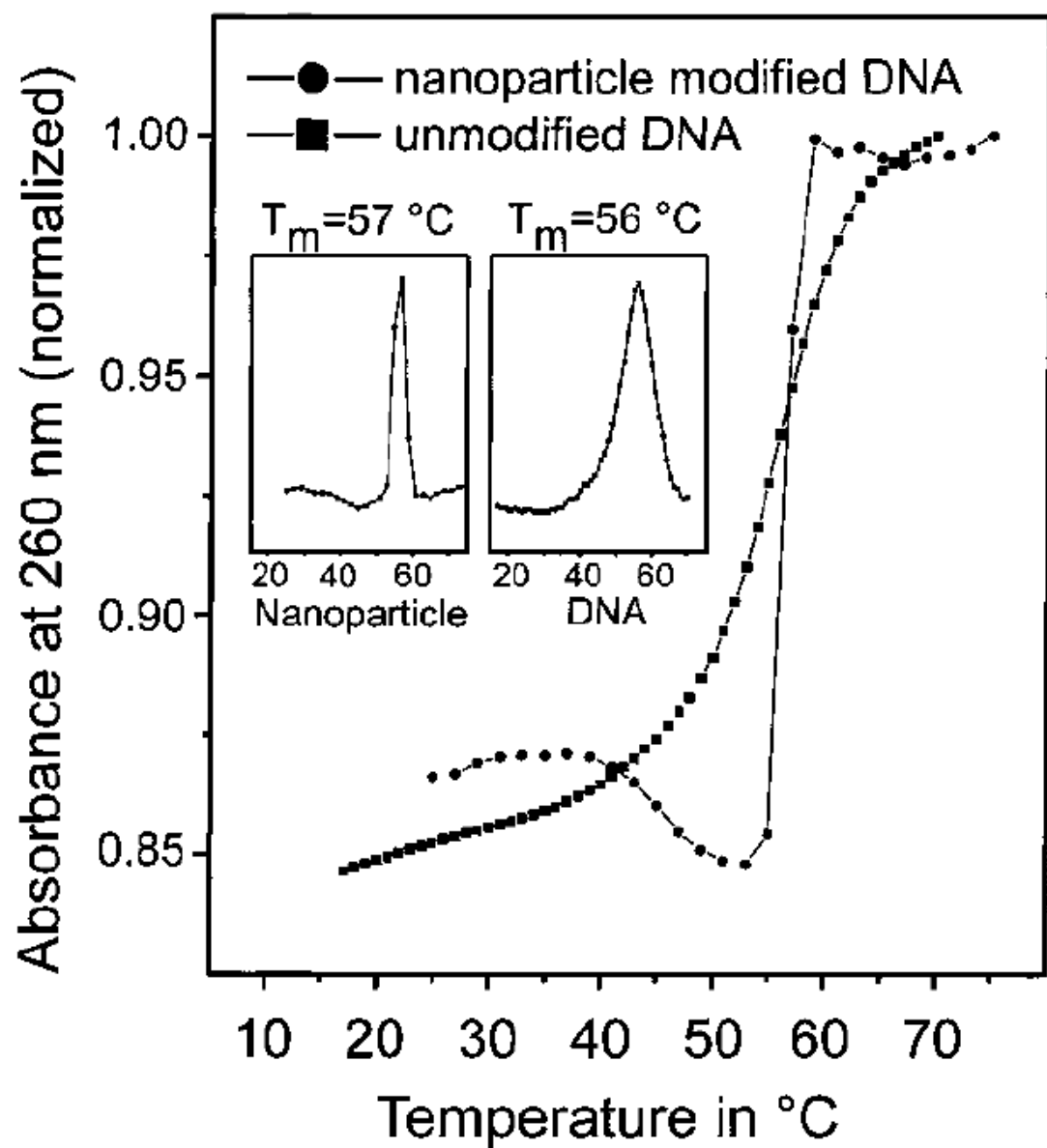
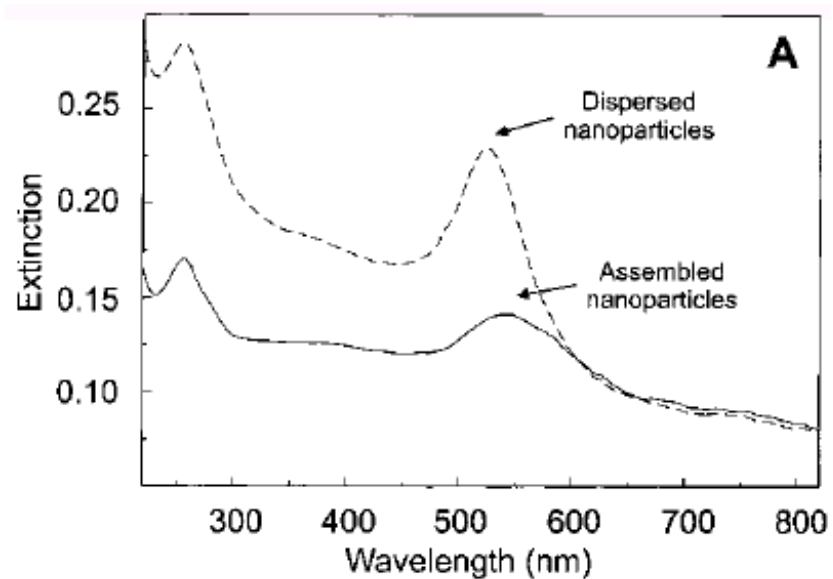
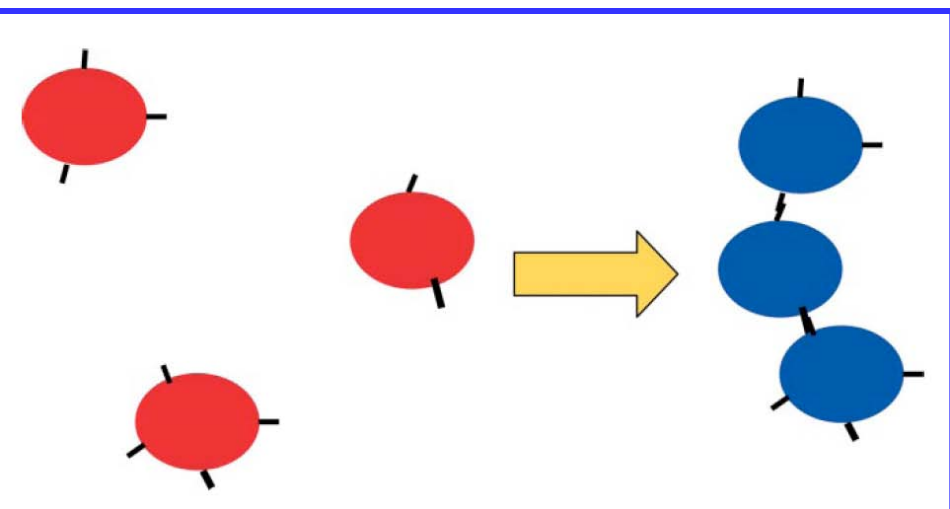


Δ↑↓ Further oligomerization and settling



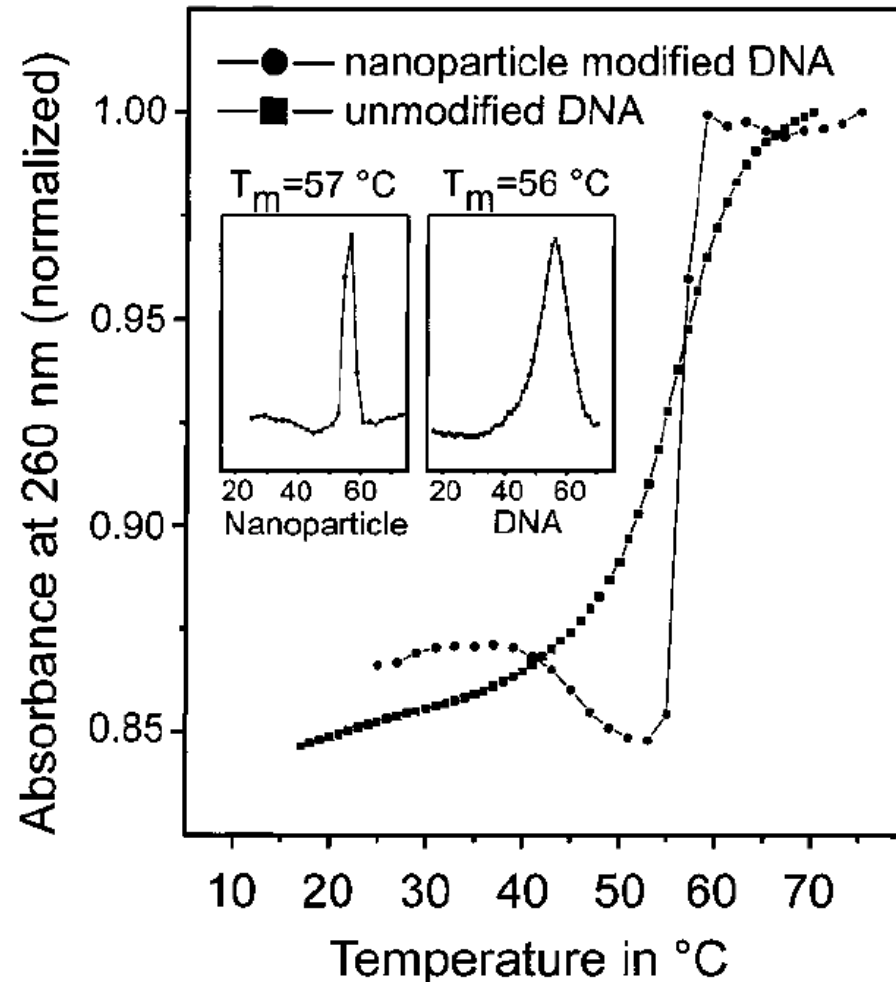
A nanoparticle “satellite structure” comprised of a 31 nm Au nanoparticle linked through DNA hybridization to several 8 nm Au nanoparticles,



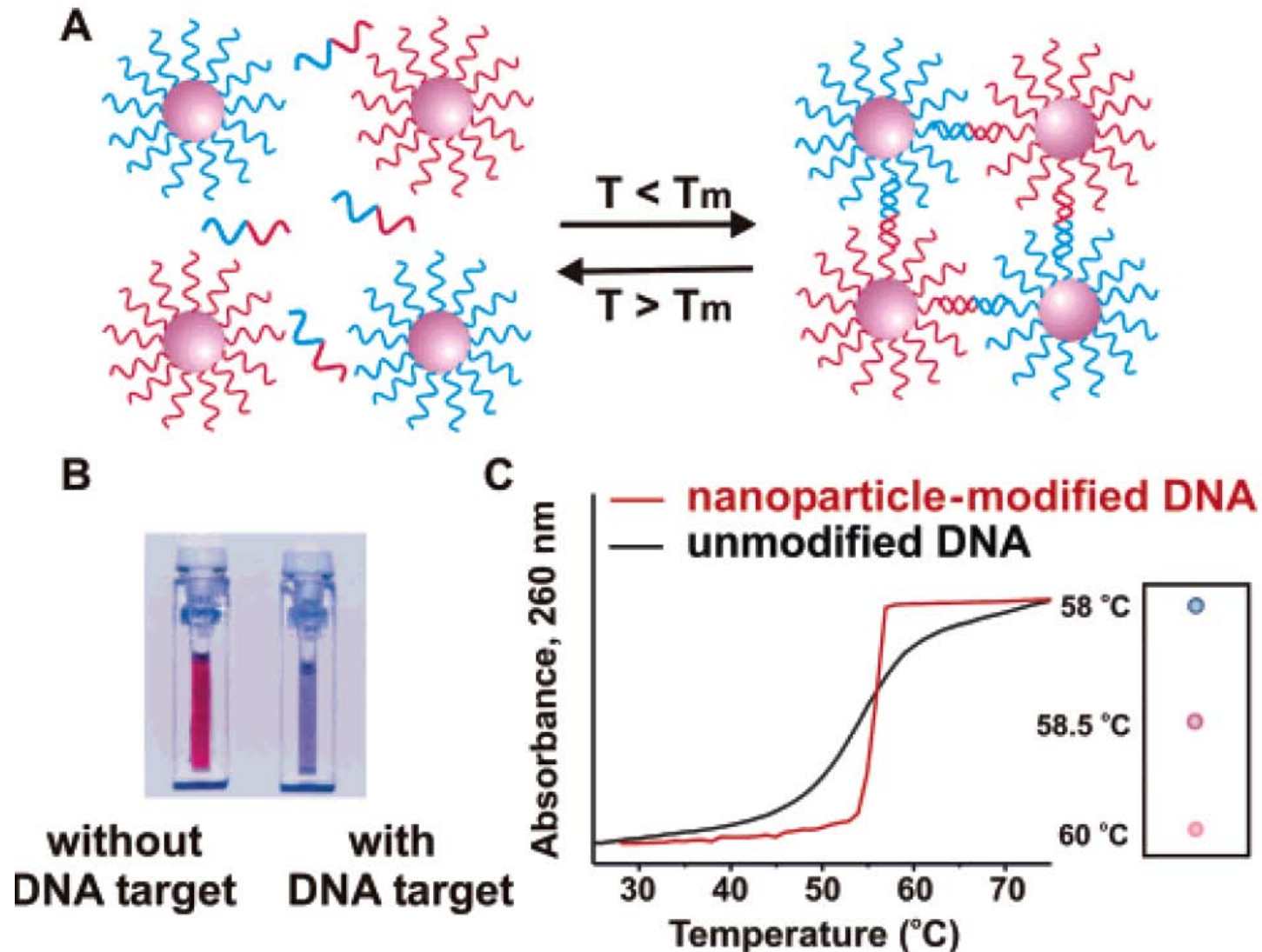


Sharp melting behavior of DNA-linked nanoparticles

- (1) the formation of an aggregate with many different DNA interconnects
- (2) the use of a nanoparticle optical signature rather than a DNA optical signature to map out the melting behavior of the aggregates.



In the presence of complementary target DNA, oligonucleotide-functionalized gold nanoparticles will aggregate.



Magnetic relaxation switches capable of sensing molecular interactions

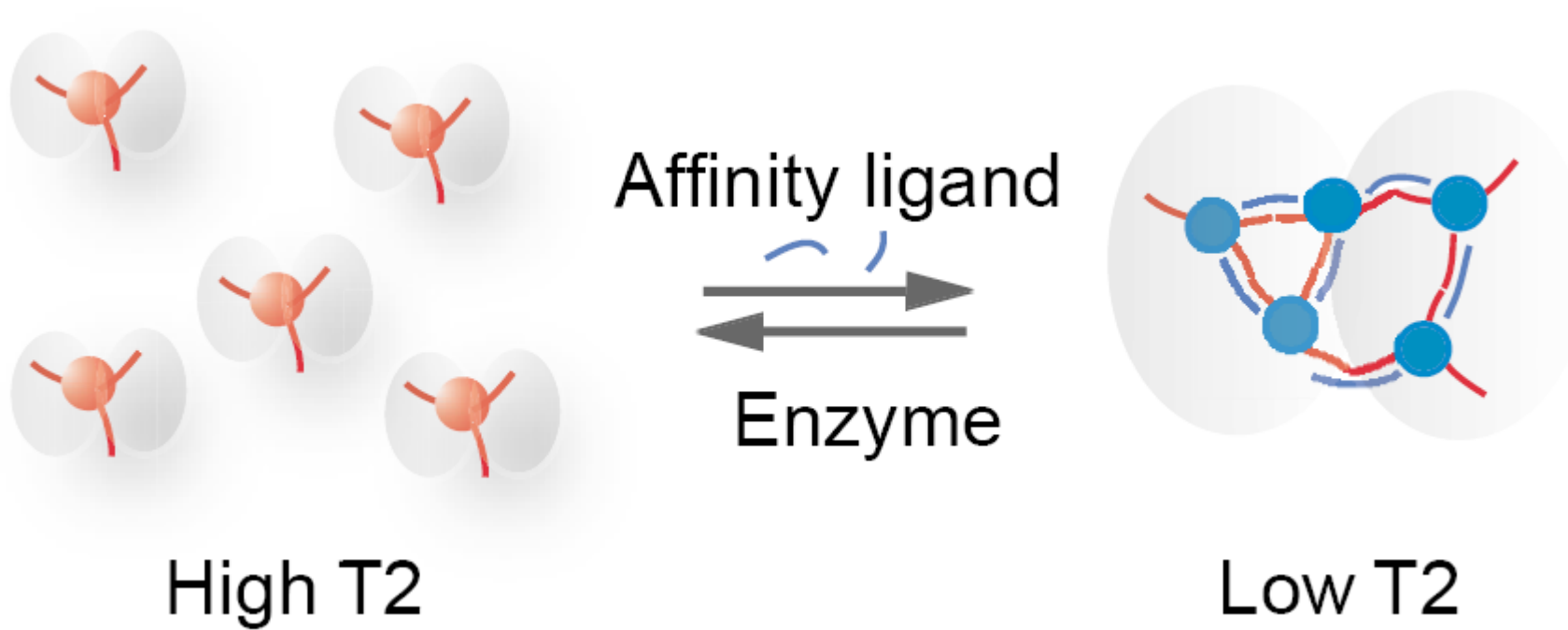
Lee Josephson, and Ralph Weissleder*

***Nature Biotech.* 2002, 20, 816.**

- Detect molecular interactions in the reversible self-assembly of disperse magnetic nanoparticles into stable assemblies
- 4 different molecular interactions:
DNA-DNA, protein-protein, protein-small molecule, enzyme reactions
- MRI detectable in turbid media
- Potential in vivo imaging

Working principle of MRS

- During this cooperative process, the superparamagnetic iron oxide core of individual nanoparticles becomes more efficient at dephasing the spins of surrounding water protons,
- Enhancing spin-spin relaxation times (T2 relaxation times)



DNA hybridization generates assembly of CLIO
→ Lowers T2

Solution color changes from **red** to **blue** upon the analyte-directed **aggregation of gold nanoparticles**, a consequence of interacting particle surface plasmons and aggregate scattering properties.

Melting profiles of the nanoparticle-labeled DNA aggregates were **extraordinarily sharp**, occurring over a temperature range much more narrow than the transition for unlabeled or conventional fluorophore-labeled DNA.

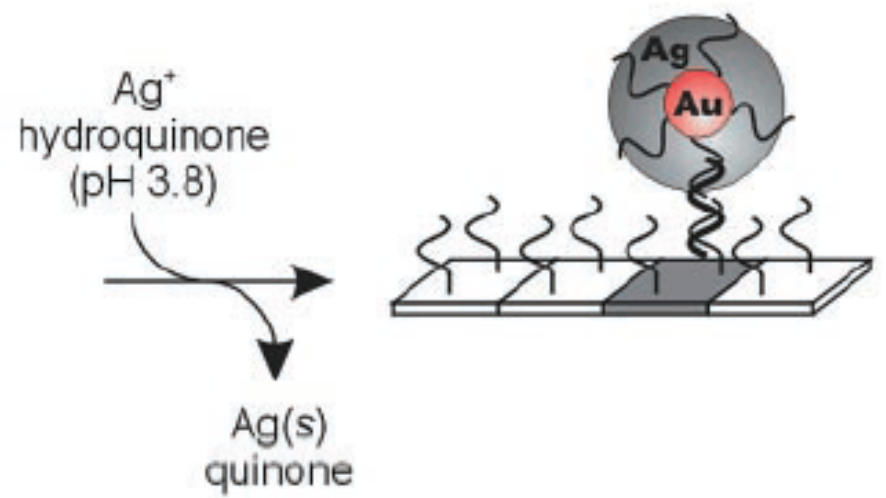
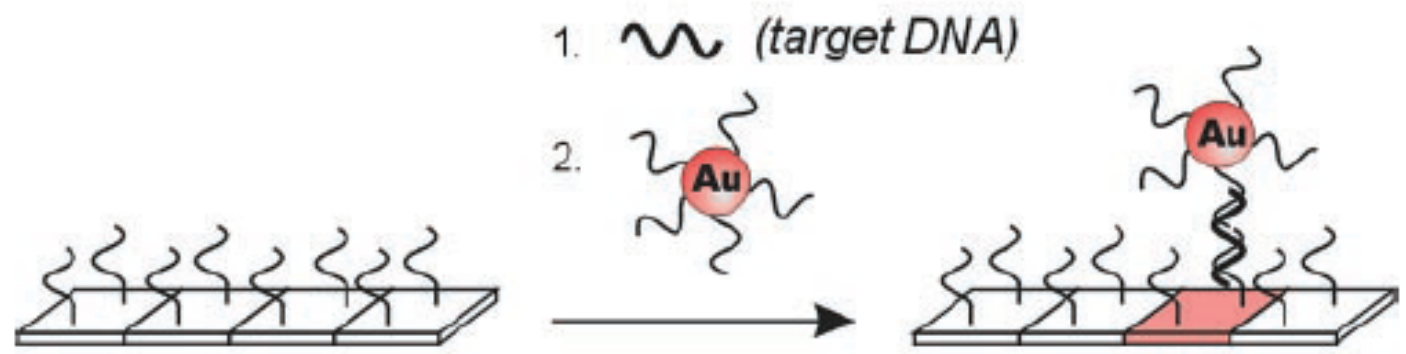
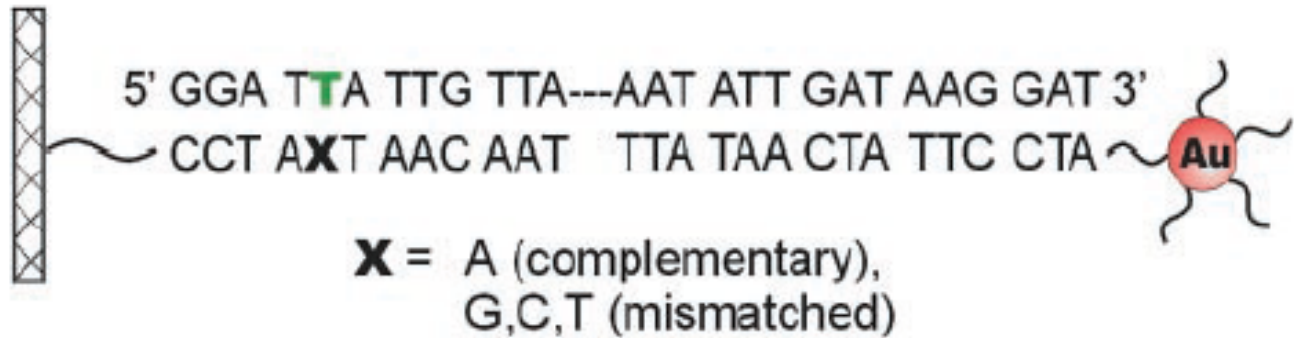
By virtue of sharp melting transitions target DNA could be differentiated from DNA with single base-pair mismatches simply by measuring absorbance (or looking at color) as a function of temperature.

Scanometric DNA Array Detection with Nanoparticle Probes

T. Andrew Taton,^{1,2} Chad A. Mirkin,^{1,2*} Robert L. Letsinger^{1*}
Science **2000**, 289, 1757.

- Specific hybridization of surface-bound, single strand capture oligonucleotides to complementary targets.
- Both the specificity and sensitivity of these assays are dependent on the dissociation properties of capture strands hybridized to perfect and to mismatched complements.
- These network structures exhibit exceptionally sharp melting profiles; FWHM as low as 2°C.
- Sharp melting transitions allow one to differentiate a perfectly complementary target strand from a strand with a single base mismatch

- Analyzing combinatorial DNA arrays using oligonucleotide-modified gold nanoparticle probes
- Melting profiles of the targets from an array substrate.
- Discrimination of an oligonucleotide sequence from targets with single nucleotide mismatches with a selectivity that is over three times that observed for fluorophore-labeled targets.
- When coupled with a signal amplification method based on nanoparticle-promoted reduction of silver(I), the sensitivity of this scanometric array detection system exceeds that of the analogous fluorophore system by two orders of magnitude.





A



B



C

(10 nM)



D



E



F

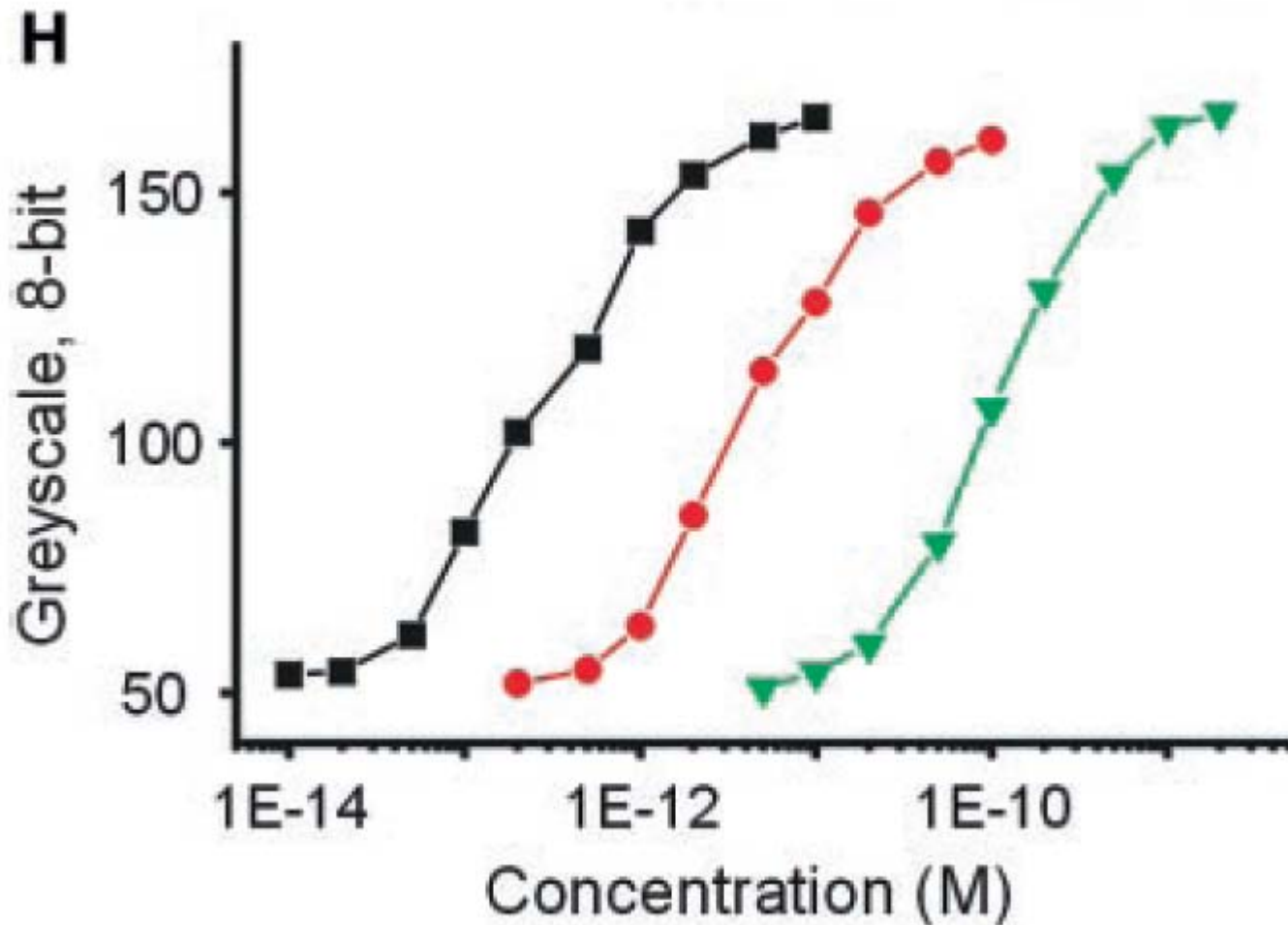
(100 pM)



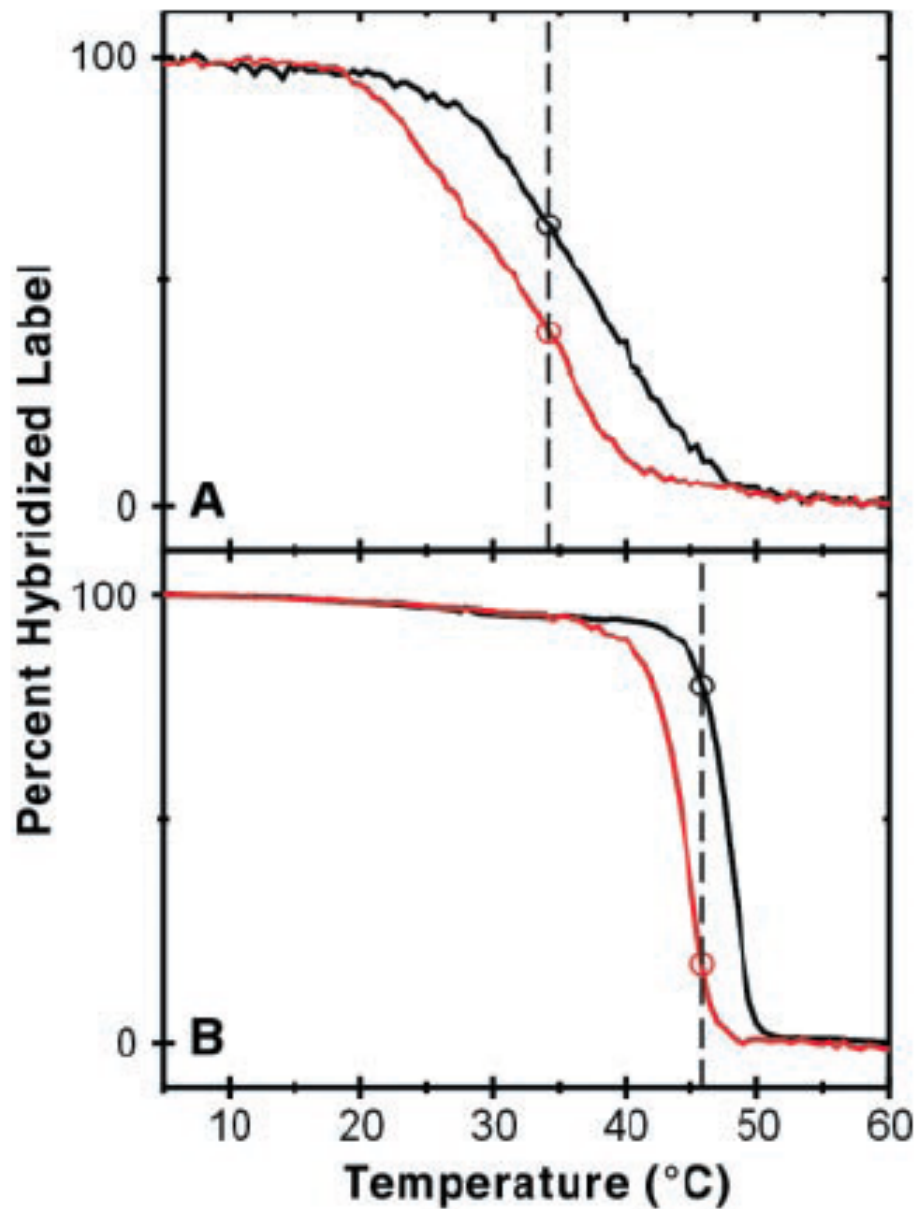
G

(control)

The lowest target concentration that can be effectively distinguished from the background baseline is 50 fM.

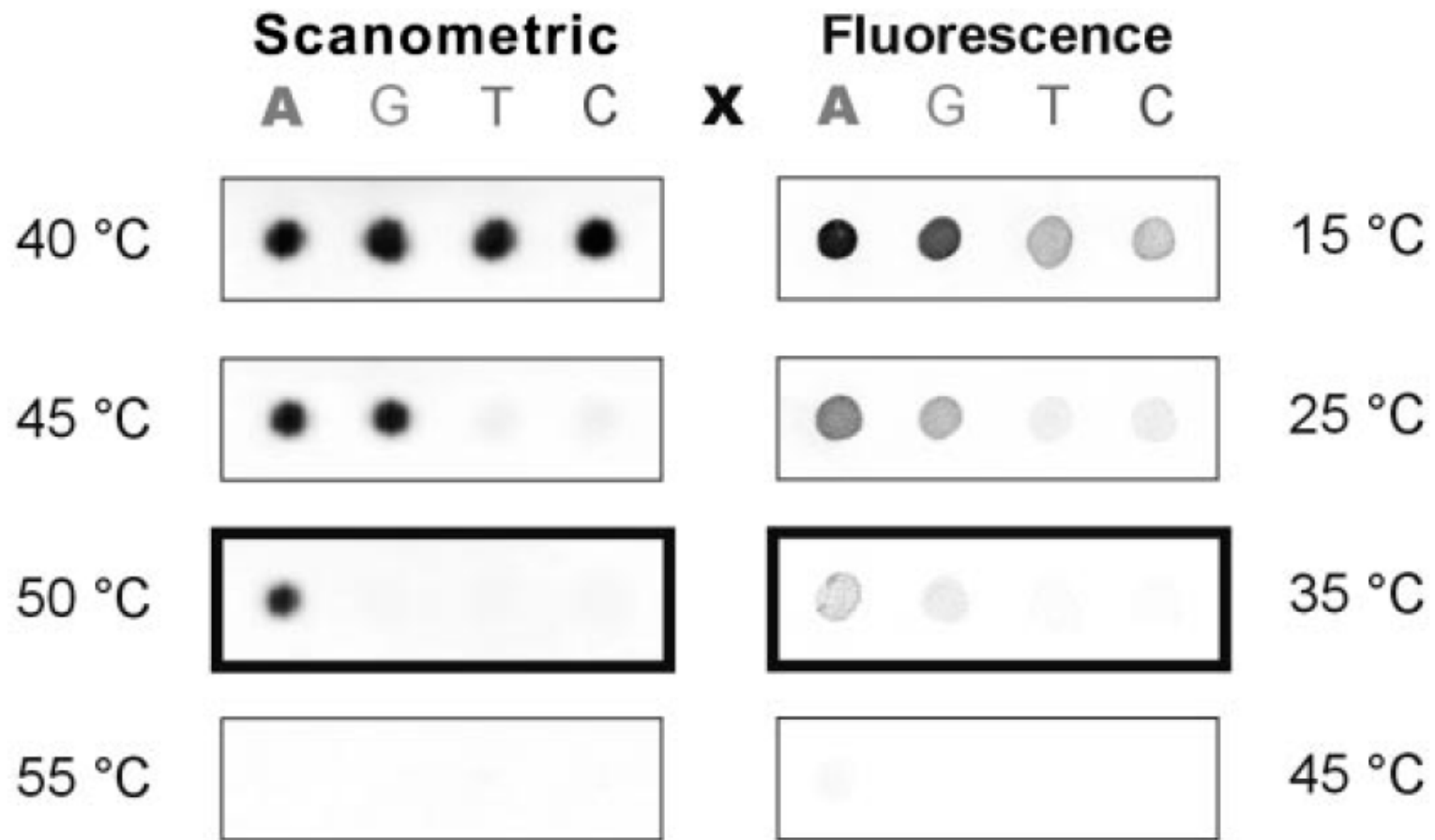


Melting curves for relative selectivity



FWHM of 18 C

3 C



Hybridization signal could be resolved at the X 5 A elements at target concentrations as low as 50 fM (5); this represents a 100-fold increase in sensitivity over that of Cy3-labeled arrays imaged by confocal fluorescence microscopy, for which target concentrations of > 5 pM required

“Northwestern Spot Test” for polynucleotide detection

